

## 10.1 INTRODUCTION

Resonant circuits can be either the lumped-element type, made by combining separate capacitors and inductors, which are small compared with a wavelength, or distributed, as was seen for sections of transmission line in Chapter 5. In a lumped-element circuit, a capacitor is used for storage of electric energy and an inductor stores magnetic energy; at the resonant frequency, there is an exchange of energy between the inductor and the capacitor every quarter-cycle. There is also an exchange between electric and magnetic energies every quarter-cycle in the distributed resonant circuit. In this case, however, the same region is used for both energies, rather than having separate components for each type.

Distributed resonant circuits utilize the resonant properties of standing waves set up by interference between forward and reverse traveling waves on transmission structures and, hence, are generally of a size comparable with a wavelength. This idea was introduced in Sec. 5.13 for a shorted transmission line with length equal to a multiple of a quarter-wavelength. Some closed metal cavities can be understood as sections of transmission structures with short-circuited ends and therefore containing standing waves. Strip-type structures such as microstrip, used in microwave and millimeter-wave circuits, make light, compact resonant transmission-type structures. A solid dielectric-cylinder resonator can be made using a section of a dielectric rod transmission structure (Sec. 9.2).

Not all resonators are simple enough in shape to be considered as sections of a wave-guiding system, and for these, other methods of solving the boundary value problem are required. We shall see some small-gap cavities that are particularly useful for electron devices. Some of these may be considered as capacitively loaded transmission lines. In others, the electric and magnetic energies are effectively separated so they may be considered as lumped  $L$ - $C$  circuits, with the one-turn inductor providing the self-shielding.

The oscillating energy is introduced by a probe or other means of coupling to the resonant structure. If the energy is provided by the probe at one of the many resonant frequencies, the impedance seen by the input probe is real. If the energy coupled in is greater than the losses in each cycle, the oscillating waves will increase in amplitude until the losses just equal the energy supplied. Losses take place in the surfaces of the metals, in any dielectrics present, and, in open structures, through radiation. If the source

excites the structure at a frequency somewhat off resonance, the energies in electric and magnetic fields do not balance. Some extra energy must be supplied over one part of the cycle and it is given back to the source during another part of the cycle; thus, the line acts as a reactive load on the exciting source, in addition to a resistive component representing the small losses. The similarity to ordinary tuned-circuit operation is evident, and as with such circuits, the concept of  $Q$  is useful in describing the effect of losses on bandwidth.

## Resonators of Simple Shape

### 10.2 FIELDS OF SIMPLE RECTANGULAR RESONATOR

For the first mode to be studied in some detail, we shall choose that mode in a rectangular conducting box which may be considered the standing wave pattern corresponding to the  $TE_{10}$  mode in a rectangular guide. As was done in the study of waveguides, the conducting walls will be taken as perfect, and losses in an actual resonator will be computed approximately by taking the current flow of the ideal mode as flowing in the walls of known conductivity.

In the rectangular conducting box of Fig. 10.2a, imagine a  $TE_{10}$  waveguide mode oriented with its electric field in the  $y$  direction and propagating in the  $z$  direction. The condition that  $E_y$  shall be zero at  $z = 0$  and  $d$ , as required by the perfect conductors, is satisfied if the dimension  $d$  is a half-guide wavelength. Using Eq. 8.8(11),

$$d = \frac{\lambda_g}{2} = \frac{\lambda}{2\sqrt{1 - (\lambda/2a)^2}}$$

Then the resonant frequency is

$$f_0 = \frac{v}{\lambda} = \frac{\sqrt{a^2 + d^2}}{2ad\sqrt{\mu\epsilon}} \quad (1)$$

To obtain the field distribution in the dielectric interior, we add positive and negative propagating waves of the form of Eqs. 8.8(4) and 8.8(5)

$$E_y = (E_+ e^{-j\beta z} + E_- e^{j\beta z}) \sin \frac{\pi x}{a} \quad (2)$$

$$H_x = -\frac{1}{Z_{TE}} (E_+ e^{-j\beta z} - E_- e^{j\beta z}) \sin \frac{\pi x}{a} \quad (3)$$

$$H_z = \frac{j}{\eta} \left( \frac{\lambda}{2a} \right) (E_+ e^{-j\beta z} + E_- e^{j\beta z}) \cos \frac{\pi x}{a} \quad (4)$$

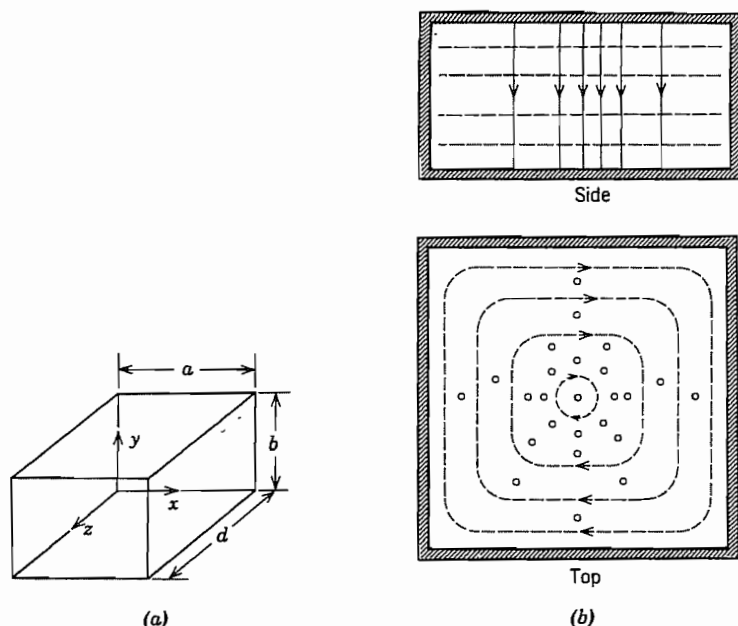


**FIG. 10.2** (a) Rectangular cavity. (b) Electric and magnetic fields in rectangular resonator with  $TE_{101}$  mode. Solid lines represent electric field, and dashed lines, magnetic field.

Since  $E_y$  must be zero at  $z = 0$ ,  $E_- = -E_+$ , as we would expect, since the reflected wave from the perfectly conducting wall should be equal to the incident wave.  $E_y$  must also be zero at  $z = d$ , so that  $\beta = \pi/d$ . Then (2)–(4) may be simplified, letting  $E_0 = -2jE_+$ :

$$E_y = E_0 \sin \frac{\pi x}{a} \sin \frac{\pi z}{d} \quad (5)$$

$$H_x = -j \frac{E_0}{\eta} \frac{\lambda}{2d} \sin \frac{\pi x}{a} \cos \frac{\pi z}{d} \quad (6)$$

$$H_z = j \frac{E_0}{\eta} \frac{\lambda}{2a} \cos \frac{\pi x}{a} \sin \frac{\pi z}{d} \quad (7)$$

In studying the foregoing expressions, we find that electric field passes vertically from top to bottom, entering top and bottom normally and becoming zero at the side walls as required by the perfect conductors. The magnetic field lines lie in horizontal  $x$ - $z$  planes and surround the vertical displacement current resulting from the time rate of change of  $E_y$ . Fields are sketched roughly in Fig. 10.2b. There are equal and opposite charges on top and bottom because of the normal electric field ending there. A current flows between top and bottom, becoming vertical in the side walls. Here we are re-

mind of a conventional resonant circuit, with the top and bottom acting as capacitor plates and the side walls as the current path between them. In the lumped-element circuit, electric and magnetic fields are separated, whereas here they are intermingled.

Because the mode studied here has one half-sine variation in the  $x$  direction, none in the  $y$  direction, and one in the  $z$  direction, it is sometimes known as a  $TE_{101}$  mode. The coordinate system is of course arbitrary, but some choice must be made before the mode can be described in this manner.

### 10.3 ENERGY STORAGE, LOSSES, AND $Q$ OF A RECTANGULAR RESONATOR

The energy storage and energy loss in the rectangular resonator of the preceding section are quantities of fundamental interest. Since the total energy passes between electric and magnetic fields, we may calculate it by finding the energy storage in electric fields at the instant when these are a maximum, for magnetic fields are then zero in the standing wave pattern of the resonator:

$$U = (U_E)_{\max} = \frac{\epsilon}{2} \int_0^d \int_0^b \int_0^a |E_y|^2 dx dy dz$$

Utilizing Eq. 10.2(5), we see that

$$\begin{aligned} U &= \frac{\epsilon}{2} \int_0^d \int_0^b \int_0^a E_0^2 \sin^2 \frac{\pi x}{a} \sin^2 \frac{\pi z}{d} dx dy dz \\ &= \frac{\epsilon E_0^2}{2} \cdot \frac{a}{2} \cdot b \cdot \frac{d}{2} = \frac{\epsilon abd}{8} E_0^2 \end{aligned} \quad (1)$$

To obtain an approximation for power loss in the walls, we utilize the current flow in the ideal conductors as obtained from the tangential magnetic field at the surface. Referring to Fig. 10.2*a*,

$$\begin{array}{ll} \text{Front:} & J_{sy} = -H_x|_{z=d} \\ \text{Back:} & J_{sy} = H_x|_{z=0} \\ \text{Left side:} & J_{sy} = -H_z|_{x=0} \\ \text{Right side:} & J_{sy} = H_z|_{x=a} \\ \text{Top:} & J_{sx} = -H_z, J_{sz} = H_x \\ \text{Bottom:} & J_{sx} = H_z, J_{sz} = -H_x \end{array}$$

If the conducting walls have surface resistivity  $R_s$ , the foregoing currents will produce losses as follows:

$$\begin{aligned} W_L &= \frac{R_s}{2} \left\{ 2 \int_0^b \int_0^a |H_x|_{z=0}^2 dx dy + 2 \int_0^d \int_0^b |H_z|_{x=0}^2 dy dz \right. \\ &\quad \left. + 2 \int_0^d \int_0^a [|H_x|^2 + |H_z|^2] dx dz \right\} \end{aligned}$$

In this equation, the first term comes from the front and back, the second from the left and right sides, and the third from top and bottom. Substituting from Eqs. 10.2(6) and

10.2(7) and evaluating the integrals,

$$W_L = \frac{R_s \lambda^2}{8\eta^2} E_0^2 \left[ \frac{ab}{d^2} + \frac{bd}{a^2} + \frac{1}{2} \left( \frac{a}{d} + \frac{d}{a} \right) \right] \quad (2)$$

The  $Q$  of the resonator may be defined from the basic definition of Eq. 5.14(4):

$$Q = \frac{\omega_0 U}{W_L} \quad (3)$$

Substituting (1) and (2) with  $\lambda$  from Eq. 10.2(1), we have

$$Q = \frac{\pi\eta}{4R_s} \left[ \frac{2b(a^2 + d^2)^{3/2}}{ad(a^2 + d^2) + 2b(a^3 + d^3)} \right] \quad (4)$$

Note that for a cube,  $a = b = d$ , this reduces to the expression

$$Q_{\text{cube}} = \frac{\sqrt{2}\pi}{6} \frac{\eta}{R_s} = 0.742 \frac{\eta}{R_s} \quad (5)$$

For an air dielectric,  $\eta \approx 377 \, \Omega$ , and for a copper conductor at 10 GHz,  $R_s \approx 0.0261 \, \Omega$ , the  $Q$  is about 10,730. Thus we see the very large values of  $Q$  for such resonators as compared with those for lumped circuits (order of a few hundred) or even with resonant lines (order of a few thousand). In practice, some care must be used if  $Q$ 's of the order of that calculated are to be obtained, since disturbances caused by the coupling system, surface irregularities, and other perturbations will act to increase the losses. Dielectric losses and radiation from small holes, when present, may be especially serious in lowering the  $Q$ .

It will be shown in Chapter 11 that a lumped circuit model applies to a cavity mode in the vicinity of resonance. From it we can deduce that the  $Q$ , defined in terms of stored energy and power loss, is also useful in estimating bandwidth of the cavity just as for the lumped resonant circuit. If  $\Delta f$  is the distance between points on the response curve for which amplitude response is down to  $1/\sqrt{2}$  of its maximum value (Sec. 5.14),

$$\frac{\Delta f}{f_0} \approx \frac{1}{Q} \quad (6)$$

Thus, for the foregoing, a  $Q$  of 10,000 in a cavity resonant at 10 GHz will yield a bandwidth between "half-power" points of 1 MHz.

## 10.4 OTHER MODES IN THE RECTANGULAR RESONATOR

As has been noted, the particular mode studied for the rectangular box is only one of an infinite number of possible modes. If we adopt the point of view that a resonant mode is the standing wave pattern for incident and reflected waveguide modes, any one of the infinite number of possible waveguide waves might be used, with any integral

number of half-waves between shorting ends. We recognize that this description of a particular field pattern is not unique, for it depends on the axis chosen to be the "direction of propagation" for the waveguide modes. Thus (see Prob. 10.2b) the simple mode studied in past sections would be a  $TE_{101}$  mode if the  $z$  axis or  $x$  axis were considered the direction of propagation, but it would be a  $TM_{110}$  mode if the vertical ( $y$ ) axis were taken as the propagation direction. In the following, a coordinate system will be chosen as in Fig. 10.2a, and field patterns will be obtained by superposing incident and reflected waves for various waveguide modes propagating in the  $z$  direction.

**The  $TE_{mnp}$  Mode** If we select the  $TE_{mnp}$  mode of a rectangular waveguide (see Sec. 8.7), addition of positively and negatively traveling waves for  $H_z$  gives

$$H_z = (Ae^{-j\beta z} + Be^{j\beta z}) \cos \frac{m\pi x}{a} \cos \frac{n\pi y}{b}$$

Since the normal component of magnetic field,  $H_z$ , must be zero at  $z = 0$  and  $z = d$ , then  $B = -A$  and  $\beta d = p\pi$  with  $p$  an integer. Let  $C = -2jA$ .

$$\begin{aligned} H_z &= A(e^{-j\beta z} - e^{j\beta z}) \cos \frac{m\pi x}{a} \cos \frac{n\pi y}{b} \\ &= C \cos \frac{m\pi x}{a} \cos \frac{n\pi y}{b} \sin \frac{p\pi z}{d} \end{aligned} \quad (1)$$

Then, substituting (1) in Eqs. 8.2(13)–(16), remembering that for the negatively traveling waves all terms multiplied by  $\beta$  change sign,

$$\begin{aligned} H_x &= -\frac{j\beta}{k_c^2} (Ae^{-j\beta z} - Be^{j\beta z}) \left(-\frac{m\pi}{a}\right) \sin \frac{m\pi x}{a} \cos \frac{n\pi y}{b} \\ &= -\frac{C}{k_c^2} \left(\frac{p\pi}{d}\right) \left(\frac{m\pi}{a}\right) \sin \frac{m\pi x}{a} \cos \frac{n\pi y}{b} \cos \frac{p\pi z}{d} \end{aligned} \quad (2)$$

$$H_y = -\frac{C}{k_c^2} \left(\frac{p\pi}{d}\right) \left(\frac{n\pi}{b}\right) \cos \frac{m\pi x}{a} \sin \frac{n\pi y}{b} \cos \frac{p\pi z}{d} \quad (3)$$

$$E_x = \frac{j\omega\mu C}{k_c^2} \left(\frac{n\pi}{b}\right) \cos \frac{m\pi x}{a} \sin \frac{n\pi y}{b} \sin \frac{p\pi z}{d} \quad (4)$$

$$E_y = -\frac{j\omega\mu C}{k_c^2} \left(\frac{m\pi}{a}\right) \sin \frac{m\pi x}{a} \cos \frac{n\pi y}{b} \sin \frac{p\pi z}{d} \quad (5)$$

where  $\beta = \frac{p\pi}{d}$  and, from Eq. 8.2(18),

$$k_c^2 = \left(\frac{m\pi}{a}\right)^2 + \left(\frac{n\pi}{b}\right)^2 \quad (6)$$

From (6) and Eq. 8.2(19) we find the resonant frequency:

$$f_0 = \frac{1}{2\pi\sqrt{\mu\epsilon}} \left[ \left( \frac{m\pi}{a} \right)^2 + \left( \frac{n\pi}{b} \right)^2 + \left( \frac{p\pi}{d} \right)^2 \right]^{1/2} \quad (7)$$

**The  $TM_{mnp}$  Mode** In a similar manner, positively and negatively traveling  $TM_{mn}$  modes in a rectangular waveguide may be combined to yield

$$E_z = D \sin \frac{m\pi x}{a} \sin \frac{n\pi y}{b} \cos \frac{p\pi z}{d} \quad (8)$$

$$E_x = -\frac{D}{k_c^2} \left( \frac{p\pi}{d} \right) \left( \frac{m\pi}{a} \right) \cos \frac{m\pi x}{a} \sin \frac{n\pi y}{b} \sin \frac{p\pi z}{d} \quad (9)$$

$$E_y = -\frac{D}{k_c^2} \left( \frac{p\pi}{d} \right) \left( \frac{n\pi}{b} \right) \sin \frac{m\pi x}{a} \cos \frac{n\pi y}{b} \sin \frac{p\pi z}{d} \quad (10)$$

$$H_x = \frac{j\omega\epsilon D}{k_c^2} \left( \frac{n\pi}{b} \right) \sin \frac{m\pi x}{a} \cos \frac{n\pi y}{b} \cos \frac{p\pi z}{d} \quad (11)$$

$$H_y = -\frac{j\omega\epsilon D}{k_c^2} \left( \frac{m\pi}{a} \right) \cos \frac{m\pi x}{a} \sin \frac{n\pi y}{b} \cos \frac{p\pi z}{d} \quad (12)$$

The quantity  $k_c^2$  and resonant frequency  $f_0$  are as in (6) and (7).

**General Comments** We note first that TM and TE modes of the same order  $m, n, p$  have identical resonant frequencies. Such modes with different field patterns but the same resonant frequency are known as *degenerate* modes. Other cases of degeneracy may exist as in a cube,  $a = b = d$ , where orders 112, 121, and 211 of both TM and TE types have the same resonant frequency.

It is also apparent from (7) that, as the order of a mode becomes higher for a given box size, the resonant frequency increases. Put differently, it means that to be resonant at a given frequency, the box must be made bigger as the order increases. This is to be expected, since more half-sine waves are to fit in each dimension. It can be shown (Probs 10.4b and 10.4c) that  $Q$  increases at a given frequency as one goes to higher mode orders. This too is logical, since the larger box has a greater volume-to-surface ratio, and energy is stored in the volume, whereas it is lost on the imperfectly conducting surface. The high-order modes are consequently useful in "echo boxes" where a high  $Q$  is desired so that the energy will decay at a very slow rate after being excited by a pulse.

## 10.5 CIRCULAR CYLINDRICAL RESONATOR

For a circular cylindrical resonator (Fig. 10.5) there is a simple mode analogous to that first studied for the rectangular box (Sec. 10.2). The vertical electric field has a maxi-

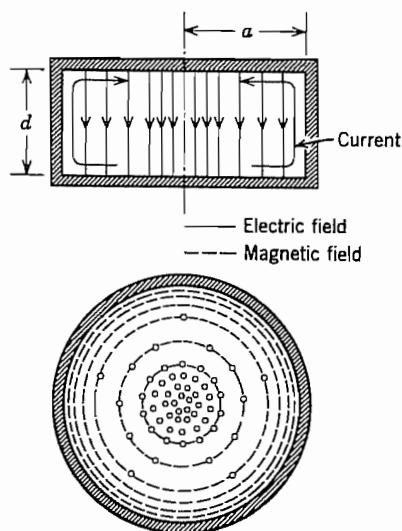


**FIG. 10.5** Sections through a cylindrical cavity with fields of  $TM_{010}$  mode. Convention is as in Table 8.9.

imum at the center and dies off to zero at the conducting side walls. A circumferential magnetic field surrounds the displacement current represented by the time-varying electric field. Neither component varies in the axial or circumferential direction. Equal and opposite charges exist on the two end plates, and a vertical current flows in the side walls. The mode may be considered a  $TM_{01}$  mode in a circular waveguide operating at cutoff (to give the constancy with respect to  $z$ ), or it may be thought of as the standing wave pattern produced by inward and outward radially propagating waves of the radial transmission line type (Sec. 9.3). From either point of view we obtain the field components

$$E_z = E_0 J_0(kr) \quad (1)$$

$$H_\phi = \frac{jE_0}{\eta} J_1(kr) \quad (2)$$

$$k = \frac{p_{01}}{a} = \frac{2.405}{a} \quad (3)$$

Then the resonant frequency is

$$f_0 = \frac{k}{2\pi\sqrt{\mu\epsilon}} = \frac{2.405}{2\pi a\sqrt{\mu\epsilon}} \quad (4)$$

The energy stored in the cavity at resonance may be found from the energy in the electric fields at the instant these have their maximum value. Take  $a$  and  $d$ , respectively,



as radius and length of the cavity:

$$U = d \int_0^a \frac{\epsilon |E_z|^2}{2} 2\pi r dr = \pi \epsilon d E_0^2 \int_0^a r J_0^2(kr) dr$$

This may be integrated by Eq. 7.15(22):

$$U = \pi \epsilon d E_0^2 \frac{a^2}{2} J_1^2(ka) \quad (5)$$

If the walls are of imperfect conductors, the power loss may be calculated approximately:

$$W_L = 2\pi a d \frac{R_s}{2} |J_{sz}|^2 + 2 \int_0^a \frac{R_s}{2} |J_{sr}|^2 2\pi r dr$$

The first term represents losses on the side wall, the second on top and bottom. The current per unit width  $J_{sr}$  on top and bottom is  $\pm H_\phi$ , and  $J_{sz}$  on the side wall is the value of  $H_\phi$  at  $r = a$ . Substituting from (2), we see that

$$W_L = \pi R_s \left[ ad \frac{E_0^2}{\eta^2} J_1^2(ka) + 2 \int_0^a \frac{E_0^2}{\eta^2} r J_1^2(kr) dr \right]$$

This may also be integrated by Eq. 7.15(22), recalling that  $J_0(ka) = 0$  is the condition for resonance:

$$W_L = \frac{\pi a R_s E_0^2}{\eta^2} J_1^2(ka) [d + a] \quad (6)$$

The  $Q$  of the mode may then be obtained as usual from power losses (6) and energy stored (5), using (4) for resonant frequency:

$$Q = \frac{\omega_0 U}{W_L} = \frac{\eta}{R_s} \frac{p_{01}}{2(a/d + 1)} \quad (7)$$

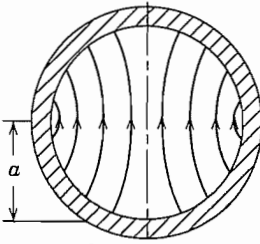
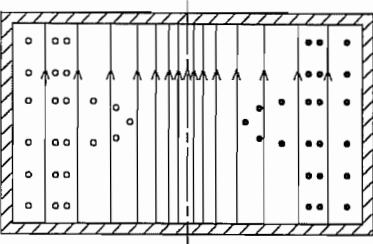
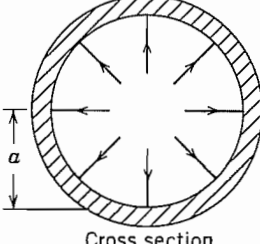
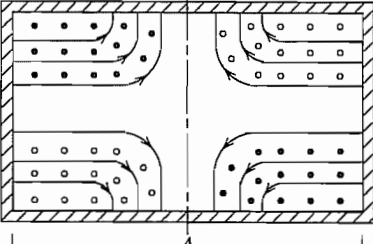
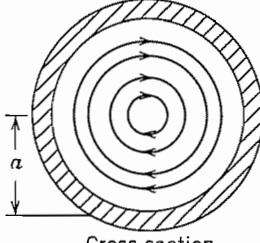
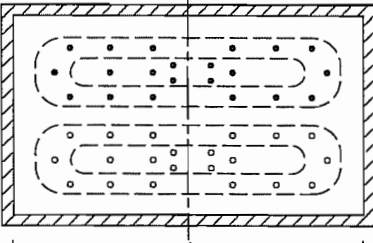
where

$$p_{01} \approx 2.405$$

An infinite number of additional modes may be obtained for the cylindrical resonator by considering others of the possible waveguide modes for circular cylindrical guides as propagating in the axial direction with an integral number of half guide wavelengths between end plates. In this manner the standing wave pattern formed by the superposition of incident and reflected waves fulfills the boundary conditions of the conducting ends. Table 10.5 shows a  $TE_{11}$  mode, a  $TM_{01}$  mode, and a  $TE_{01}$  mode, each with one half guide wavelength between ends. The resonant wavelengths shown are obtained by solving the equation

$$d = \frac{p\lambda_g}{2} = \frac{p\lambda}{2} \left[ 1 - \left( \frac{\lambda}{\lambda_c} \right)^2 \right]^{-1/2} \quad (8)$$

Table 10.5

<p>TE<sub>111</sub>, Cylinder</p>  <p>Cross section through A-A</p>		$f_0 = \frac{c}{2l\sqrt{\mu_r\epsilon_r}} \sqrt{1 + \left(\frac{2l}{3.41a}\right)^2}$
<p>TM<sub>011</sub>, Cylinder</p>  <p>Cross section through A-A</p>		$f_0 = \frac{c}{2l\sqrt{\mu_r\epsilon_r}} \sqrt{1 + \left(\frac{2l}{2.61a}\right)^2}$
<p>TE<sub>011</sub>, Cylinder</p>  <p>Cross section through A-A</p>		$f_0 = \frac{c}{2l\sqrt{\mu_r\epsilon_r}} \sqrt{1 + \left(\frac{2l}{1.64a}\right)^2}$

The corresponding resonant frequencies are shown in the table. For these modes the integer  $p$  is unity in (8), and cutoff wavelength  $\lambda_c$  is obtained from Sec. 8.9. Note that in the designations TE<sub>111</sub>, TM<sub>011</sub>, TE<sub>011</sub>, the order of subscripts is not in the cyclic order of coordinates,  $r$ ,  $\phi$ ,  $z$ , since it is common in circular waveguides to designate the  $\phi$  variation by the first subscript.

Of the foregoing modes, the TE<sub>011</sub> is perhaps the most interesting since it has only circumferential currents in both the cylindrical wall and the end plates. Thus, if a resonator for such a wave is tuned by moving the end plate, one does not need a good contact between the ends and the cylindrical wall since no current flows between them.

For both of the other modes shown (and in fact all except those of type  $TE_{0np}$ ) a finite current does flow between the cylinder and its ends so that any sliding contact must be good to prevent serious loss.

As with the rectangular resonator, it would be found that higher wave orders (those having more variations with any or all coordinates  $r, \phi, z$ ) would require larger resonators to be resonant at a given frequency. The  $Q$  would become higher because of the increased volume-to-surface ratio, but the modes would become close together in frequency relative to the resonant frequency so that it might be difficult to excite one mode only.

## 10.6 STRIP RESONATORS

Strip-type resonant structures are used in microwave and millimeter-wave circuits as single resonant elements and as components in filters. Such structures are light and compact, though more limited in power-handling capability than the box resonators discussed in the preceding sections. The quality factor  $Q$  of this kind of resonator is limited by losses in the conductors and dielectric, and is also decreased by radiation, since they are open structures. The examples shown here are of the common microstrip configuration (Sec. 8.6), with the strips on a dielectric substrate coated on the opposite side with a metallic ground plane, but similar arrangements can be used with the coplanar configurations.

Figure 10.6a shows a microstrip resonator equivalent to the resonant transmission line with short-circuited ends described in Sec. 5.13. To satisfy the boundary conditions at the ends, the strip length  $l$  must be

$$l = n\lambda_g/2 \quad (1)$$

where  $\lambda_g = v_p/f = \lambda_0/\sqrt{\epsilon_{\text{eff}}}$  and  $n$  is an integer. We assume negligible variation of the fields across the strip.

Short circuits in microstrip require connections ("vias") through the dielectric, so a more common and convenient arrangement is to leave the ends of the strip open, rather than shorted. Again,  $l = n\lambda_g/2$  in the simple model that assumes ideal open circuits at the ends. However, there are fringing fields at the ends and these can be represented by an added length  $\Delta l$  so that the resonance condition is

$$l + 2\Delta l = n\lambda_g/2 \quad (2)$$

The value of  $\Delta l$  in the usual situation where the dielectric and ground plane extend beyond the end of the strip has been found by numerical methods. Practical calculations can be made from empirical formulas that have been fit to the results of the calculations. The following formula is accurate to about 5% for  $0.3 < w/d < 2$  and  $1 < \epsilon_r < 50$ :<sup>1</sup>

$$\frac{\Delta l}{d} = 0.412 \frac{(\epsilon_{\text{eff}} + 0.3)[(w/d) + 0.262]}{(\epsilon_{\text{eff}} - 0.258)[(w/d) + 0.813]} \quad (3)$$

<sup>1</sup> R. K. Hoffmann, *Handbook of Microwave Integrated Circuits*, Artech House, Norwood, MA, 1987.

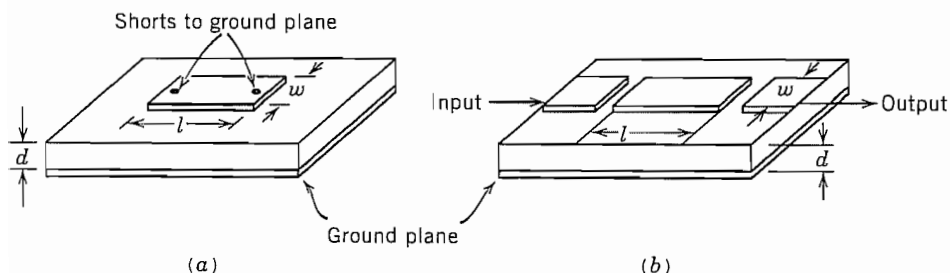


**Fig. 10.6** (a) Microstrip resonator with short-circuited ends. (b) Open-circuited microstrip resonator showing capacitively coupled input and output.

where  $w$  is the strip width,  $d$  is the dielectric thickness, and  $\epsilon_{\text{eff}}$  is defined as in Sec. 8.6. Figure 10.6b shows an open-circuit resonator with capacitively coupled input and output connections.

Another important form of strip-type structure is the microstrip ring resonator shown in Fig. 10.6c. There are no end effects and, if the curvature is not too great, the mean circumference is an integral number of wavelengths at resonance. Thus,

$$l = 2\pi r_{\text{aver}} = n\lambda_g \quad (4)$$

Because of the curvature of the line, radiation is a more important source of loss than in straight-line resonators. Excitation in this example is by distributed coupling to an adjacent straight section of microstrip, though capacitive coupling as in Fig. 10.6b can be used.

Strip-type resonators can also be made in the form of rectangular or circular patches, normally with open sides as shown in Figs. 10.6d and e. Note that the rectangular patch differs from the strip in Fig. 10.6b by having width comparable with wavelength. If the edges are open circuits, resonance in the rectangular patch is as in the rectangular box cavity in Secs. 10.2–10.4, except with open-circuit (zero tangential  $\mathbf{H}$ ) boundary conditions. Only modes with nonzero  $E_z$  and no variations in the  $z$  direction can be accommodated in the strip-type structure. Thus, the modes are the  $\text{TM}_{mnp}$  types in Eqs. 10.4(8)–(12) with  $p = 0$ :

$$E_z = E_0 \cos k_x x \cos k_y y \quad (5)$$

$$H_x = \frac{k_y}{j\omega\mu} E_0 \cos k_x x \sin k_y y \quad (6)$$

$$H_y = -\frac{k_x}{j\omega\mu} E_0 \sin k_x x \cos k_y y \quad (7)$$

with  $k_x = m\pi/(a + \Delta a)$  and  $k_y = n\pi/(b + \Delta b)$ . Here,  $\Delta a$  and  $\Delta b$  account for fringing, and may be estimated from (3). In this case the empirical formula, adapted from the limiting case of the end of a very wide strip,  $w/d \rightarrow \infty$ , is<sup>1</sup>

$$\Delta a/d \text{ (or } \Delta b/d) = 2(1.35/\epsilon_r + 0.44) \quad (8)$$

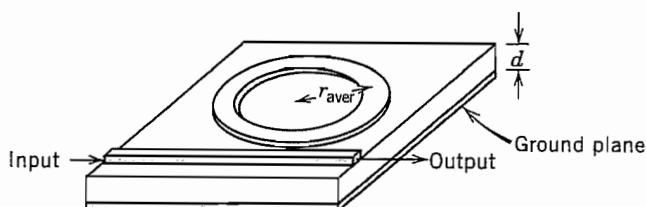


**FIG. 10.6c** Microstrip ring resonator with distributed coupling.

The resonance condition can be adapted from Eq. 10.4(7) with  $p = 0$ :

$$f_0 = \frac{1}{2\pi\sqrt{\mu\epsilon}} \left[ \left( \frac{m\pi}{a + \Delta a} \right)^2 + \left( \frac{n\pi}{b + \Delta b} \right)^2 \right] \quad (9)$$

As in the case of the rectangular patch resonator, a variety of resonant modes exist in the circular patch resonator. The simplest of these is the lowest-order azimuthally symmetric radial-transmission-line mode, assuming an open circuit at  $r = a + \Delta a$ . Since  $a$  is the radius, the  $\Delta a/d$  here is one-half the value in (8). The fields are described by Bessel functions as in the pillbox resonator of Fig. 10.5:

$$E_z = E_0 J_0(kr) \quad (10)$$

$$H_\phi = \frac{jE_0}{\eta} J_1(kr) \quad (11)$$

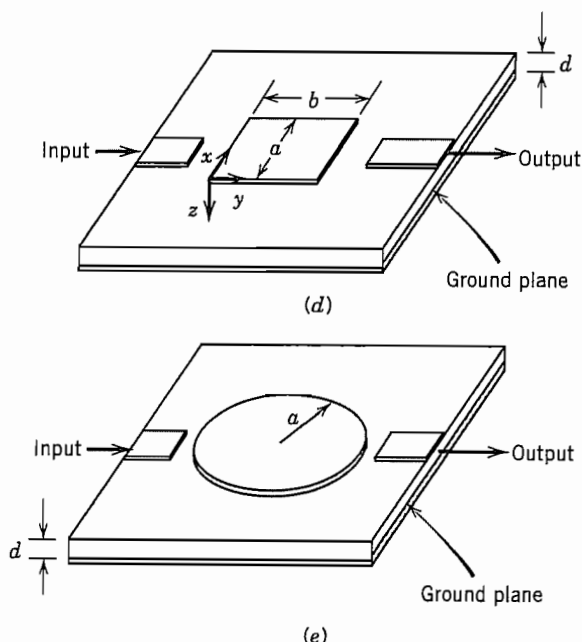


**FIG. 10.6** (d) Rectangular patch resonator in microstrip technology. (e) Circular microstrip patch resonator.

With an open circuit at  $a + \Delta a$ , the tangential field  $H_\phi$  must vanish there, so the resonance condition is

$$f_0 = \frac{1}{2\pi\sqrt{\mu\epsilon}} k_0 = \frac{1}{2\pi\sqrt{\mu\epsilon}} \frac{p_{11}}{a + \Delta a} \quad (12)$$

where  $p_{11} = 3.832$  is the first root of the Bessel function  $J_1$ .

More generally, the modes in the circular patch may be considered analytically the same as  $\text{TM}_{n1}$  waveguide modes (Sec. 8.9) at cutoff where there is no  $z$  variation ( $\beta = 0$ ), except that here the open-circuit boundary condition at the edge radius must be applied. From Eqs. 8.9(8)–(10),

$$E_z = E_0 J_n(k_c r) \cos n\phi \quad (13)$$

$$H_\phi = -j \frac{\omega\epsilon}{k_c} E_0 J'_n(k_c r) \cos n\phi \quad (14)$$

$$H_r = -\frac{j\omega\epsilon n}{k_c^2 r} E_0 J_n(k_c r) \cos n\phi \quad (15)$$

Resonance is at that frequency  $f_0$  where  $k = k_c$ , or  $f_0 = k_c/2\pi\sqrt{\mu\epsilon}$ . The cutoff wavenumber  $k_c$  is given by Eq. 8.9(12) except that instead of  $p_{n1}$ , which are the roots of the Bessel function in (13), we must use the roots of its derivative,  $p'_{n1}$  (see Table 7.15b). Thus, the resonant frequency is

$$f_0 = \frac{p'_{n1}}{2\pi(a + \Delta a)\sqrt{\mu\epsilon}} \quad (16)$$

The mode with the lowest resonant frequency is  $\text{TM}_{110}$ , where the third subscript indicates no variation in the  $z$  direction. This mode does not have azimuthal symmetry. Its resonant frequency is

$$f_0 = \frac{1.841}{2\pi(a + \Delta a)\sqrt{\mu\epsilon}} \quad (17)$$

which is lower than that of the lowest-order symmetric mode (12).

All of the common methods of exciting the patch resonators indicated in Figs. 10.6d and e are asymmetric, so one should expect the asymmetric modes to be preferentially excited.

The factors that contribute to the  $Q$ 's of these resonators are conductor losses, which are proportional to the surface resistance  $R_s$ , dielectric losses, which are proportional to the loss factor  $\tan \delta_\epsilon$  of the dielectric, radiation losses, and excitation of spurious resonances. Radiation losses can be minimized by enclosing the structure in a metal box, and dielectric losses are usually less than those in the conductors. For high values of  $Q$  associated with the various loss mechanisms, they are nearly independent and can be combined as

$$Q = \left( \frac{1}{Q_c} + \frac{1}{Q_d} + \frac{1}{Q_r} \right)^{-1} \quad (18)$$

where the subscripts refer to conductor, dielectric, and radiation, respectively. Each  $Q$  in (18) is given by  $Q = \omega_0 U / W_L$ . Energy loss  $W_L$  in the conductors can be calculated as for the box cavities, i.e., integration of Eq. 3.18(5) over the metal surfaces. The dielectric energy loss is found by integrating the density,  $W_{Ld} = \omega_0 \epsilon'' E^2 / 2$ , where  $E$  is electric field, over the volume of the resonator.

Procedures for calculating radiation loss are found in the literature.<sup>1</sup> Energy storage  $U$  is calculated as for the box cavities. With normal metals, the  $Q$ 's are much lower than for box cavities, typically 100 to 1000 for copper or gold on any of several different dielectrics at room temperature. Strip-type resonators of the same configurations but made with superconductors have  $Q$ 's 10 to 100 times higher at 10 GHz. The advantage of using superconductors is greatest at microwave ( $< 20$  GHz) frequencies, and decreases at higher frequencies because of the difference of frequency dependencies of  $R_s$  shown in Fig. 3.16b.

### 10.7 WAVE SOLUTIONS IN SPHERICAL COORDINATES

Spherical resonators are of more intellectual than practical interest, but will serve to introduce wave solutions in spherical coordinates. In this section we develop such solutions. We shall sketch here only those solutions with axial symmetry,  $\partial/\partial\phi = 0$ . The solutions with general  $\phi$  variations are more involved, but have been given completely by Stratton.<sup>2</sup> It is found that with axial symmetry the solutions separate into waves with components  $E_r, E_\theta, H_\phi$  and those with components  $H_r, H_\theta, E_\phi$ . These are called TM and TE types, respectively, the spherical surface  $r$  constant serving here as the transverse surface.

Consider then TM spherical modes with axial symmetry by setting  $\partial/\partial\phi = 0$  in Maxwell's equations in spherical coordinates. The three curl equations containing  $E_r, E_\theta, H_\phi$  are

$$\frac{\partial}{\partial r}(rE_\theta) - \frac{\partial E_r}{\partial \theta} = -j\omega\mu(rH_\phi) \quad (1)$$

$$\frac{1}{r \sin \theta} \frac{\partial}{\partial \theta}(H_\phi \sin \theta) = j\omega\epsilon E_r \quad (2)$$

$$-\frac{\partial}{\partial r}(rH_\phi) = j\omega\epsilon(rE_\theta) \quad (3)$$

Equations (2) and (3) may be differentiated and substituted in (1), leading to an equation in  $H_\phi$  alone:

$$\frac{\partial^2}{\partial r^2}(rH_\phi) + \frac{1}{r^2} \frac{\partial}{\partial \theta} \left[ \frac{1}{\sin \theta} \frac{\partial}{\partial \theta}(rH_\phi \sin \theta) \right] + k^2(rH_\phi) = 0 \quad (4)$$

<sup>2</sup> J. A. Stratton, *Electromagnetic Theory*, Chap. VII, McGraw-Hill, New York, 1941.

To solve this partial differential equation, we follow the product solution technique. Assume

$$(rH_\phi) = R\Theta \quad (5)$$

where  $R$  is a function of  $r$  alone, and  $\Theta$  is a function of  $\theta$  alone. If this is substituted in (4), the functions of  $r$  may be separated from the functions of  $\theta$ , and these must then be separately equal to a constant if they are to equal each other for all values of  $r$  and  $\theta$ . For a definitely ulterior motive, we label this constant  $n(n+1)$ :

$$\frac{r^2 R''}{R} + k^2 r^2 = -\frac{1}{\Theta} \frac{d}{d\theta} \left[ \frac{1}{\sin \theta} \frac{d}{d\theta} (\Theta \sin \theta) \right] = n(n+1) \quad (6)$$

Thus there are two ordinary differential equations, one in  $r$  only and one in  $\theta$  only. Let us consider that in  $\theta$  first, making the substitutions

$$u = \cos \theta, \quad \sqrt{1-u^2} = \sin \theta, \quad \frac{d}{d\theta} = -\sin \theta \frac{d}{du}$$

Then

$$(1-u^2) \frac{d^2 \Theta}{du^2} - 2u \frac{d\Theta}{du} + \left[ n(n+1) - \frac{1}{1-u^2} \right] \Theta = 0 \quad (7)$$

The differential equation (7) is reminiscent of Legendre's equation (Sec. 7.18) and is in fact a standard form. This form is

$$(1-x^2) \frac{d^2 y}{dx^2} - 2x \frac{dy}{dx} + \left[ n(n+1) - \frac{m^2}{1-x^2} \right] y = 0 \quad (8)$$

One of the solutions is written<sup>3</sup>

$$y = P_n^m(x)$$

and the function defined by this solution is called an associated Legendre function of the first kind, order  $n$ , degree  $m$ . These are related to the ordinary Legendre functions by the equation

$$P_n^m(x) = (1-x^2)^{m/2} \frac{d^m P_n(x)}{dx^m} \quad (9)$$

As a matter of fact, (8) could be derived from the ordinary Legendre equation by this substitution. A solution to (7) may then be written

$$\Theta = P_n^1(u) = P_n^1(\cos \theta) \quad (10)$$

And, from (9),

$$P_n^1(\cos \theta) = -\frac{d}{d\theta} P_n(\cos \theta) \quad (11)$$

<sup>3</sup> A second solution,  $Q_n^m(x)$ , is needed when the axis is not included in the region of solution (Ref. 2).



Thus for integral values of  $n$  these associated Legendre functions are also polynomials consisting of a finite number of terms. By differentiations according to (9) in Eq. 7.18(8), the polynomials of the first few orders are found to be

$$\begin{aligned} P_0^1(\cos \theta) &= 0 \\ P_1^1(\cos \theta) &= \sin \theta \\ P_2^1(\cos \theta) &= 3 \sin \theta \cos \theta \\ P_3^1(\cos \theta) &= \frac{3}{2} \sin \theta (5 \cos^2 \theta - 1) \\ P_4^1(\cos \theta) &= \frac{5}{2} \sin \theta (7 \cos^3 \theta - 3 \cos \theta) \end{aligned} \quad (12)$$

Other properties of these functions that will be useful to us, and which may be found from a study of the above, are as follows:

1. All  $P_n^1(\cos \theta)$  are zero at  $\theta = 0$  and  $\theta = \pi$ .
2.  $P_n^1(\cos \theta)$  are zero at  $\theta = \pi/2$  if  $n$  is even.
3.  $P_n^1(\cos \theta)$  are a maximum at  $\theta = \pi/2$  if  $n$  is odd, and the value of this maximum is given by

$$P_n^1(0) = \frac{(-1)^{-(n-1)/2} n!}{2^{n-1} \left[ \left( \frac{n-1}{2} \right)! \right]^2} \quad n \text{ odd} \quad (13)$$

4. The associated Legendre functions have orthogonality properties similar to those of the Legendre polynomials studied previously:

$$\int_0^\pi P_l^1(\cos \theta) P_n^1(\cos \theta) \sin \theta d\theta = 0, \quad l \neq n \quad (14)$$

$$\int_0^\pi [P_n^1(\cos \theta)]^2 \sin \theta d\theta = \frac{2n(n+1)}{2n+1} \quad (15)$$

5. The differentiation formula is

$$\frac{d}{d\theta} [P_n^1(\cos \theta)] = \frac{1}{\sin \theta} [nP_{n+1}^1(\cos \theta) - (n+1) \cos \theta P_n^1(\cos \theta)] \quad (16)$$

Note that only one solution for this second-order differential equation (7) has been considered. The other solution becomes infinite on the axis, and so will not be required in solutions valid on the axis, but will be needed in problems such as the biconical antenna analysis of Sec. 12.25.

To go back to the  $r$  differential equation obtainable from (6), substitute the variable  $R_1 = R/\sqrt{r}$ :

$$\frac{d^2 R_1}{dr^2} + \frac{1}{r} \frac{dR_1}{dr} + \left[ k^2 - \frac{(n + \frac{1}{2})^2}{r^2} \right] R_1 = 0$$

By comparing with Eq. 7.14(3) it is seen that this is Bessel's differential equation of

order  $n + \frac{1}{2}$ . A complete solution may then be written

$$R_1 = A_n J_{n+1/2}(kr) + B_n N_{n+1/2}(kr) \quad (17)$$

and

$$R = \sqrt{r} R_1$$

If  $n$  is an integer, these half-integral-order Bessel functions reduce simply to algebraic combinations of sinusoids.<sup>4</sup> For example, the first few orders are

$$\begin{aligned} J_{1/2}(x) &= \sqrt{\frac{2}{\pi x}} \sin x & N_{1/2}(x) &= -\sqrt{\frac{2}{\pi x}} \cos x \\ J_{3/2}(x) &= \sqrt{\frac{2}{\pi x}} \left[ \frac{\sin x}{x} - \cos x \right] & N_{3/2}(x) &= -\sqrt{\frac{2}{\pi x}} \left[ \sin x + \frac{\cos x}{x} \right] \\ J_{5/2}(x) &= \sqrt{\frac{2}{\pi x}} \left[ \left( \frac{3}{x^2} - 1 \right) \sin x - \frac{3}{x} \cos x \right] & N_{5/2}(x) &= -\sqrt{\frac{2}{\pi x}} \left[ \frac{3}{x} \sin x + \left( \frac{3}{x^2} - 1 \right) \cos x \right] \end{aligned} \quad (18)$$

The linear combinations of the  $J$  and  $N$  functions into Hankel functions (Sec. 7.14) represent waves traveling radially inward or outward, and boundary conditions will be as found previously for other Bessel functions:

1. If the region of interest includes the origin,  $N_{n+1/2}$  cannot be present since it is infinite at  $r = 0$ .
2. If the region of interest extends to infinity, the linear combination of  $J$  and  $N$  into the second Hankel function,  $H_{n+1/2}^{(2)} = J_{n+1/2} - jN_{n+1/2}$ , must be used to represent a radially outward traveling wave.

The particular combination of  $J_{n+1/2}(kr)$  and  $N_{n+1/2}(kr)$  required for any problem may be denoted as  $Z_{n+1/2}(kr)$ , and now by combining correctly (17), (10), and (5),  $H_\phi$  is determined.  $E_r$  and  $E_\theta$  follow from (2) and (3), respectively.

$$\begin{aligned} H_\phi &= \frac{A_n}{\sqrt{r}} P_n^1(\cos \theta) Z_{n+1/2}(kr) \\ E_\theta &= \frac{A_n P_n^1(\cos \theta)}{j\omega\epsilon r^{3/2}} [nZ_{n+1/2}(kr) - krZ_{n-1/2}(kr)] \\ E_r &= -\frac{A_n n Z_{n+1/2}(kr)}{j\omega\epsilon r^{3/2} \sin \theta} [\cos \theta P_n^1(\cos \theta) - P_{n+1}^1(\cos \theta)] \end{aligned} \quad (19)$$

<sup>4</sup> Special notations for the spherical or half-integral-order Bessel functions have been introduced and are useful if one has much to do with these functions. Thus Stratton, following Morse (Vibrations and Sound, p. 246, McGraw-Hill, New York, 1936) uses  $j_n(x)$  to denote  $(\pi/2x)^{1/2} J_{n+1/2}(x)$ , and similar small letters denote other spherical Bessel and Hankel functions. Still other specialized notations have been used. Because of our limited need for spherical coordinates, we shall retain the original Bessel function forms so that standard recurrence formulas may be used.

The spherically symmetric TE modes may be obtained by the above and the principle of duality (Sec. 9.5). We then replace  $E_r$  and  $E_\theta$  by  $H_r$  and  $H_\theta$ , respectively,  $H_\phi$  by  $-E_\phi$ , and  $\epsilon$  by  $\mu$ :

$$\begin{aligned} E_\phi &= \frac{B_n}{\sqrt{r}} P_n^1(\cos \theta) Z_{n+1/2}(kr) \\ H_\theta &= -\frac{B_n P_n^1(\cos \theta)}{j\omega\mu r^{3/2}} [nZ_{n+1/2}(kr) - krZ_{n-1/2}(kr)] \\ H_r &= \frac{B_n n Z_{n+1/2}(kr)}{j\omega\mu r^{3/2} \sin \theta} [\cos \theta P_n^1(\cos \theta) - P_{n+1}^1(\cos \theta)] \end{aligned} \quad (20)$$

### 10.8 SPHERICAL RESONATORS

The general discussion of spherical waves from the preceding section will now be applied to the study of some simple modes in a hollow conducting spherical resonator. Since the origin is included within the region of the solution, the Bessel functions can only be those of first kind,  $J_{n+1/2}$ . For the lowest-order TM mode, let  $n = 1$  in Eq. 10.7(19) and utilize the definitions of Eqs. 10.7(12) and 10.7(18). Letting  $C = A_1(2k/\pi)^{1/2}$ , we then have

$$H_\phi = \frac{C \sin \theta}{kr} \left( \frac{\sin kr}{kr} - \cos kr \right) \quad (1)$$

$$E_r = -\frac{2j\eta C \cos \theta}{k^2 r^2} \left( \frac{\sin kr}{kr} - \cos kr \right) \quad (2)$$

$$E_\theta = \frac{j\eta C \sin \theta}{k^2 r^2} \left[ \frac{(kr)^2 - 1}{kr} \sin kr + \cos kr \right] \quad (3)$$

The mode may be designated  $TM_{101}$ , the subscripts here giving variations in the order  $r$ ,  $\phi$ , and  $\theta$ . Electric and magnetic field lines are sketched in Fig. 10.8a.

To obtain the resonance condition, we know that  $E_\theta$  must be zero at the radius of the perfectly conducting shell,  $r = a$ . From (3), this requires

$$\tan ka = \frac{ka}{1 - (ka)^2} \quad (4)$$

Roots of this transcendental equation may be determined numerically and the first is found at  $ka \approx 2.74$ , giving a resonant frequency of

$$f_0 \approx \frac{1}{2.29\sqrt{\mu\epsilon a}} \quad (5)$$

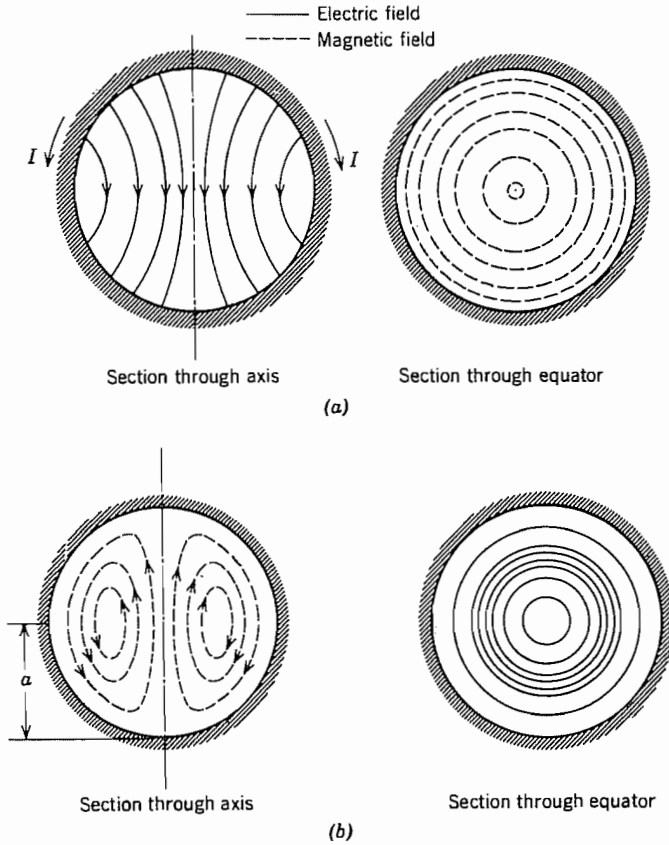


**Fig. 10.8** (a) Field patterns for  $TM_{101}$  mode in spherical resonator. (b) Field patterns for  $TE_{101}$  mode in spherical resonator.

The energy stored at resonance may be found from the peak energy in magnetic fields:

$$U = \int_0^a \int_0^\pi \frac{\mu}{2} |H_\phi|^2 2\pi r^2 \sin \theta \, d\theta \, dr$$

The value of  $H_\phi$  is given by (1), and the result of the integration may be simplified by the resonance requirement (4):

$$U = \frac{2\pi\mu C^2}{3k^3} \left[ ka - \frac{1 + (ka)^2}{ka} \sin^2 ka \right] \quad (6)$$

The approximate dissipation in conductors of finite conductivity is

$$W_L = \int_0^\pi \frac{R_s |H_\phi|^2}{2} 2\pi a^2 \sin \theta \, d\theta = \frac{4\pi R_s}{3} a^2 C^2 \sin^2 ka \quad (7)$$

So the  $Q$  of this mode is

$$Q = \frac{\eta}{2R_s(ka)^2} \left[ \frac{ka}{\sin^2 ka} - \frac{1 + (ka)^2}{ka} \right] \approx \frac{\eta}{R_s} \quad (8)$$

The “dual” of the above mode is the  $TE_{101}$  mode, and its field components may be obtained by substituting in (1) to (3)  $E_\phi$  for  $H_\phi$ ,  $-H_r$  for  $E_r$ , and  $-H_\theta$  for  $E_\theta$ . The fields are sketched in Fig. 10.8*b*. Note that the resonance condition for this mode, obtained by setting  $E_\phi = 0$  at  $r = a$ , requires

$$\tan ka = ka$$

Numerical solution of this yields  $ka \approx 4.50$ , or

$$f_0 \approx \frac{1}{1.395\sqrt{\mu\epsilon a}} \quad (9)$$

## Small-Gap Cavities and Coupling

### 10.9 SMALL-GAP CAVITIES

Because of their shielded nature and high  $Q$  possibilities, resonant cavities are ideal for use in many high-frequency tubes such as klystrons, magnetrons, and microwave triodes. When they are used with an electron stream, it is essential for efficient energy transfer that the electron transit time across the active field region be as small as possible. If resonators such as those studied in preceding sections were used, very short cylinders or prisms would be required, and  $Q$  would be low and interaction weak. Certain special shapes are consequently employed which have a small gap in the region that is to interact with the electron stream. Several examples of useful small-gap cavities will follow.

#### Example 10.9a

##### FORESHORTENED COAXIAL LINES

The structure in Fig. 10.9*a* may be considered a coaxial line  $A$  terminated in the gap capacitance  $B$  (leading to the equivalent circuit of Fig. 10.9*b*) provided that the region  $B$  is small compared with wavelength. The method is particularly useful when the region  $B$  is not uniform, but contains dielectrics or discontinuities, so long as a reasonable estimate of capacitance can be made.

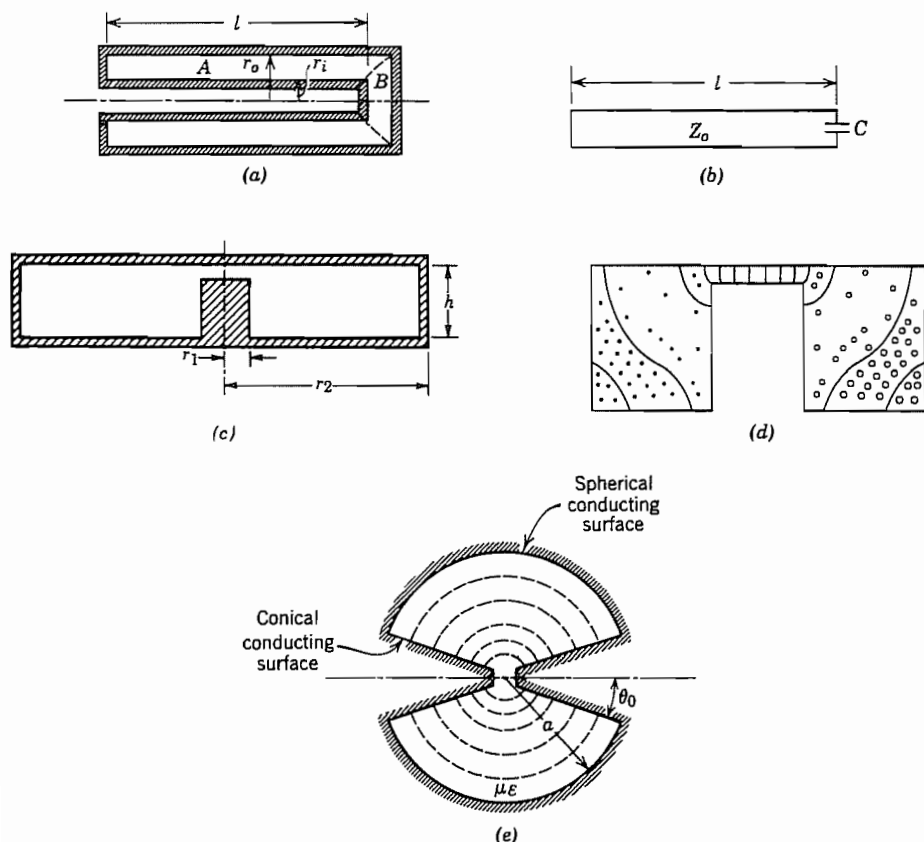


**FIG. 10.9** (a) Foreshortened coaxial-line resonator. (b) Approximate equivalent circuit for (a). (c) Foreshortened radial-line resonator. (d) Resonator intermediate between foreshortened coaxial line and foreshortened radial line. (e) Conical-line resonator.

For resonance, the reactance at any plane should be equal and opposite, looking in opposite directions. Selecting the plane of the capacitance for this purpose,

$$jZ_0 \tan \beta l = -\left(\frac{1}{j\omega_0 C}\right)$$

or

$$\beta l = \tan^{-1}\left(\frac{1}{Z_0 \omega_0 C}\right) \quad (1)$$

The resonant frequency must be found numerically from (1).

If  $C$  is small ( $Z_0 \omega_0 C \ll 1$ ), the line is practically a quarter-wave length. For larger values of  $C$ , the line is foreshortened from the quarter-wave value and would approach zero length if  $Z_0 \omega_0 C$  approached infinity.

**Example 10.9b**  
FORESHORTENED RADIAL LINES

If the proportions of the resonator are more as shown in Fig. 10.9c, it is preferable to look at the problem as one of a resonant radial transmission line (Sec. 9.3) loaded or foreshortened by the capacitance of the post or gap. Then, for resonance, the inductive reactance of the shorted radial line looking outward from radius  $r_1$  should be equal in magnitude to the capacitive reactance of the central post. Using the results and notation of Sec. 9.3 we see that

$$\frac{1}{\omega C} = -\frac{h}{2\pi r_1} Z_{01} \frac{\sin(\theta_1 - \theta_2)}{\cos(\psi_1 - \theta_2)}$$

or

$$\theta_2 = \tan^{-1} \left[ \frac{\sin \theta_1 + (2\pi r_1 / \omega C Z_{01} h) \cos \psi_1}{\cos \theta_1 - (2\pi r_1 / \omega C Z_{01} h) \sin \psi_1} \right] \quad (2)$$

Once  $\theta_2$  is found,  $kr_2$  is read from Fig. 9.3c, and resonant frequency is found from  $k$ .

**Example 10.9c**  
RESONATORS OF INTERMEDIATE SHAPE

In the coaxial-line resonator of Fig. 10.9a the electric field lines would be substantially radial in the region far from the gap. In the radial line resonator of Fig. 10.9c the electric field lines would be substantially axial in the region far from the gap. For a resonator of the same general type, but with intermediate proportions, the field lines may be transitional between these extremes as indicated in Fig. 10.9d, and neither of these approximations may yield good results. Some useful design curves for a range of proportions have been given in the literature.<sup>5</sup> Of course, if the capacitive loading at the center is great enough, the entire resonator will be relatively small compared with wavelength, and the outer portion may be considered a lumped inductance of value

$$L \approx \frac{\mu l}{2\pi} \ln \left( \frac{r_2}{r_1} \right) \quad (3)$$

Resonance is computed from this inductance and the known capacitance.

**Example 10.9d**  
CONICAL-LINE RESONATOR

A somewhat different form of small-gap resonator, formed by placing a spherical short at radius  $a$  on a conical line as studied in Sec. 9.6, is shown in Fig. 10.9e. Since this is

<sup>5</sup> T. Moreno, *Microwave Transmission Design Data*, Artech House, Norwood, MA, 1989.

a uniform line, formula (1) applies to this case as well. For the conical line,  $\beta = k$  and

$$Z_0 = \frac{\eta}{\pi} \ln \cot \frac{\theta_0}{2} \quad (4)$$

In the limit of zero capacitance (the two conical tips separated by an infinitesimal gap), the radius  $a$  becomes exactly a quarter-wavelength. The field components in this case, obtained by forming a standing wave from Eqs. 9.6(5) and 9.6(6), are

$$E_\theta = \frac{C}{\sin \theta} \frac{\cos kr}{r} \quad (5)$$

$$H_\phi = \frac{C}{j\eta \sin \theta} \frac{\sin kr}{r} \quad (6)$$

The  $Q$  of the resonator in this limiting case may be shown to be

$$Q \approx \frac{\eta\pi}{4R_s} \frac{\ln \cot (\theta_0/2)}{\ln \cot (\theta_0/2) + 0.825 \csc \theta_0} \quad (7)$$

## 10.10 COUPLING TO CAVITIES

The types of electromagnetic waves that may exist inside closed conducting cavities have been discussed without specifically analyzing ways of exciting these oscillations. Obviously they cannot be excited if the resonator is completely enclosed by conductors. Some means of coupling electromagnetic energy into and out of the resonator must be introduced from the outside. The most straightforward methods, similar to those discussed in Sec. 8.11 for exciting waves in waveguides, are:

1. Introduction of a conducting probe or antenna in the direction of the electric field lines, driven by an external transmission line
2. Introduction of a conducting loop with plane normal to the magnetic field lines
3. Introduction of a pulsating electron beam passing through a small gap in the resonator, in the direction of electric field lines, and similarly for carriers in solid-state devices
4. Introduction of a hole or iris between the cavity and a driving waveguide, the hole being located so that some field component in the cavity mode has a direction common to one in the wave mode
5. In microstrip or coplanar strip versions, coupling by adjacent strip lines as illustrated in the examples of Fig. 10.6

For example, in a velocity modulation device of the klystron type, as in Fig. 10.10a, the input cavity may be excited by a probe, the oscillations in this cavity producing a voltage across gap  $g_1$  and causing a velocity modulation of the electron beam. The velocity modulation is converted to convection current modulation by a drifting action



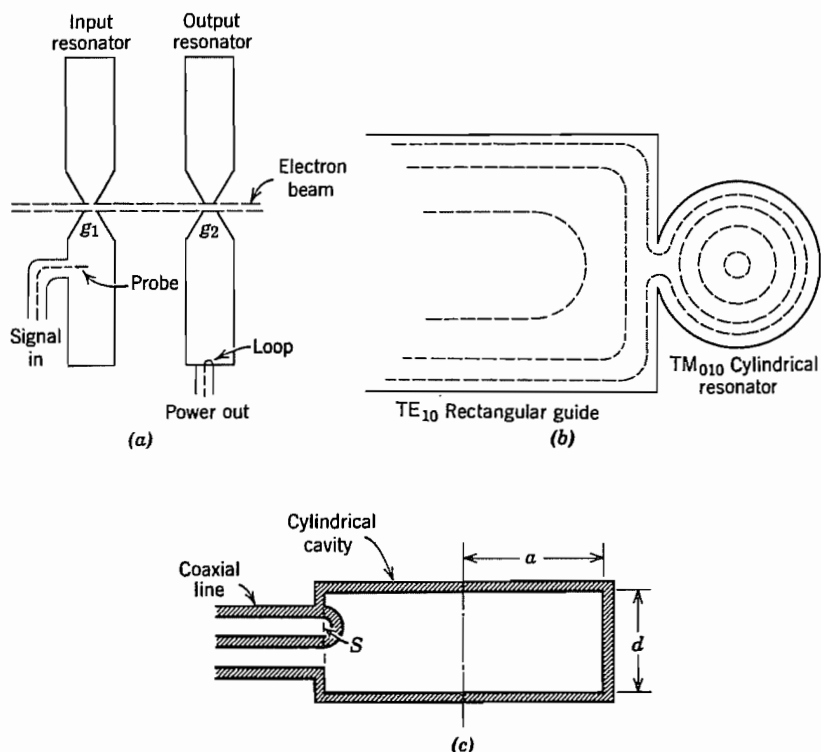


**FIG. 10.10** (a) Couplings to the cavities of a velocity modulation tube amplifier. (b) Section showing approximate form of magnetic field lines in iris coupling between a guide and cavity. (c) Magnetic coupling to a cylindrical cavity.

so that the electron beam may then excite electromagnetic oscillations in the second resonator by passing through the gap  $g_2$ . Power may be coupled out of this resonator by a coupling loop and a coaxial transmission line. Iris coupling between a  $TM_{010}$  mode in a cylindrical cavity and the  $TE_{10}$  mode in a rectangular waveguide is illustrated in Fig. 10.10b. Here the  $H_\phi$  of the cavity and the  $H_x$  of the guide are in the same direction over the hole.

The rigorous approach to a quantitative analysis of cavity coupling is given in the following chapter. Some comments and an approximate approach are, however, in order here.

### Example 10.10

#### LOOP COUPLING IN A CYLINDRICAL CAVITY

Let us concentrate on the loop coupling to a  $TM_{010}$  cylindrical mode as sketched in Fig. 10.10c. If a current is made to flow in the loop, all wave types will be excited

which have a magnetic field threading the loop. The simple  $TM_{010}$  mode is one of these, and, if it is near resonance, certainly it will be excited most. However, this wave is known to fit the boundary conditions imposed by the perfectly conducting box alone. Other waves will have to be superposed to make the electric field zero along the perfectly conducting loop, but these will in general be far from resonance and so will contribute only a reactive effect. In fact, they may be thought of as producing the self-inductance reactance of the loop, taking into account the presence of the cavity as a shield.

The voltage magnitude induced in the loop by the cavity mode is

$$|V| = \omega\mu S|H| \quad (1)$$

where  $|H|$  is magnetic field from the  $TM_{010}$  mode, averaged over the loop, and  $S$  is loop area. Consider power loss as only that from the walls, Eq. 10.5(6). This can be written in terms of magnetic field at  $r = a$  through Eq. 10.5(2):

$$W_L = \frac{\pi a(d + a)E_0^2 J_1^2(ka)R_s}{\eta^2} = \pi a(d + a)R_s|H|^2 \quad (2)$$

This loss requires an input resistance

$$R = \frac{|V|^2}{2W_L} = \frac{(\omega\mu S)^2}{2\pi a(d + a)R_s} \quad (3)$$

The reactive impedance from self-inductance of the loop,  $j\omega L$ , is added to this, but may be tuned out by a frequency shift in the cavity or by a portion of the input line as will be discussed in the following section.

## 10.11 MEASUREMENT OF RESONATOR $Q$

The  $Q$  of a cavity has been defined in terms of power loss and energy storage and has been calculated for a number of ideal configurations. It has also been noted that the  $Q$  is useful in describing bandwidth of a cavity mode, just as for a lumped-element resonant system. The reason for this is that in the vicinity of resonance for a single mode, a lumped-element equivalent circuit such as that of Fig. 10.11a is a good representation. The excitation means may excite a number of modes, but in general only one is near resonance. The elements  $G$ ,  $L$ , and  $C$  represent the mode near resonance, and  $jX$  the reactive effect of modes far from resonance. Such an equivalent circuit might be suspected to give correct qualitative results, but as will be shown in the next chapter, it actually gives useful quantitative results also. The equivalent circuit also permits one to devise ways of measuring  $Q$  when it is difficult or impossible to calculate.

Many methods of  $Q$  measurement are possible,<sup>6</sup> and commercial instruments are

<sup>6</sup> T. S. Laverghetta, Handbook of Microwave Testing, Sec. 9.2, Artech House, Norwood, MA, 1981.

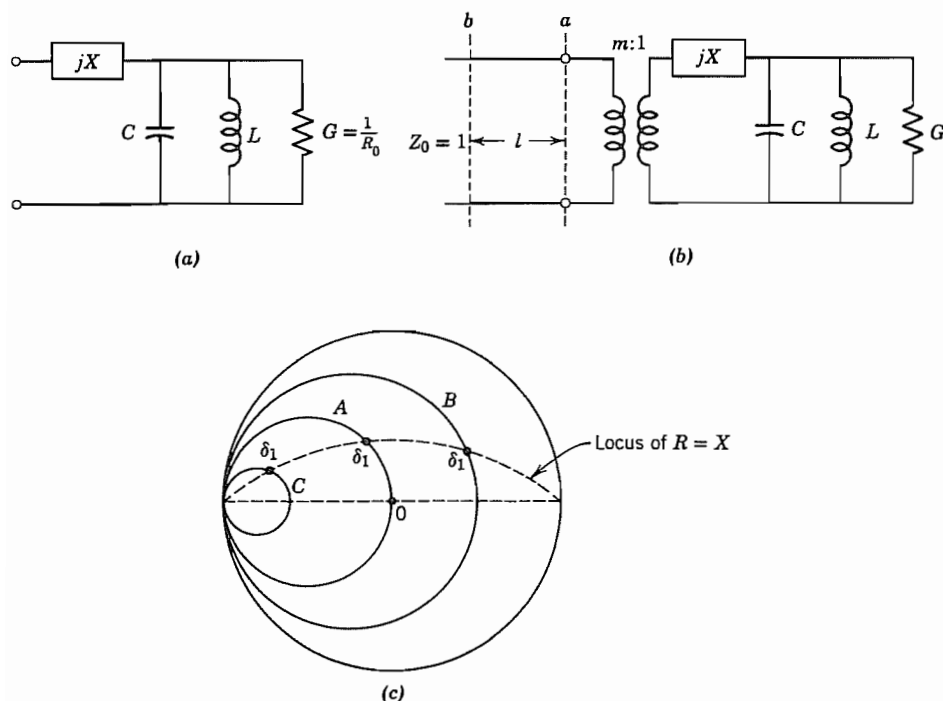


**FIG. 10.11** (a) Cavity equivalent circuit. (b) Equivalent circuit for cavity with coupling to a waveguide. (c) Locus of impedance on Smith chart for  $Q$  measurement.

available which do this directly. We shall describe a method using elemental transmission-line measurements which illustrates the use of the equivalent circuit of Fig. 10.11a and brings in the importance of the correct coupling. The coupling of the waveguide to the cavity is illustrated here by the ideal transformer of turns ratio  $m:1$  (Fig. 10.11b). The guide is assumed to have unity characteristic impedance for simplicity, so that terminating impedances are automatically normalized. The input impedance at reference  $a$  is then

$$Z_a = m^2 \left[ jX + \frac{1}{G + j(\omega C - 1/\omega L)} \right] \quad (1)$$

By defining  $Q_0 = \omega_0 C/G$ ,  $\omega_0^2 = 1/LC$ , and  $R_0 = 1/G$ , this is

$$Z_a = m^2 \left[ jX + \frac{R_0}{1 + j(\omega/\omega_0 - \omega_0/\omega)Q_0} \right] \quad (2)$$

In the vicinity of resonance,  $\omega = \omega_0(1 + \delta')$  where  $\delta'$  is small,

$$Z_a \approx jm^2X + \frac{m^2R_0}{1 + 2jQ_0\delta'} \quad (3)$$

The series reactance may be removed either by defining a new resonant frequency or by referring input to a shifted point on the waveguide. The latter is common, and the new reference may be taken as the position where the impedance seen looking toward the cavity is zero when the cavity is tuned off resonance; this is called the “detuned short” position. The detuning is sufficient to make  $Q_0\delta' \gg 1$  either by detuning the cavity (by changing  $\omega_0$ ) or by changing frequency  $\omega$ . Then, by (3),  $Z_a \approx jm^2X$  and, from the impedance transformation formula, Eq. 5.7(13), which for  $Z_0 = 1$  is

$$Z_b = \frac{Z_a + j \tan \beta l}{1 + jZ_a \tan \beta l} \quad (4)$$

we find that  $Z_b$  is zero when

$$\tan \beta l = -m^2X \quad (5)$$

The impedance  $Z_b$  at arbitrary frequencies in the neighborhood of resonance is then

$$Z_b = \frac{m^2R_{0b}}{1 + 2jQ_0\delta} \quad (6)$$

where

$$R_{0b} = R_0(1 + m^4X^2)^{-1} \quad (7)$$

and

$$\delta = \delta' - \frac{m^4XR_0}{2Q_0(1 + m^4X^2)} \quad (8)$$

The locus of impedance is measured as  $\delta'$  is varied either by changing frequency or by detuning the cavity. As impedance (6) is of the linear fraction form, it will produce a circular locus for each value of  $m^2R_{0b}$  when plotted on the Smith chart as illustrated by circles  $A$ ,  $B$ , and  $C$  in Fig. 10.11c. Circle  $A$ , for which  $m^2R_{0b} = 1$ , passes through the origin and is called the condition of *critical coupling* since it provides a perfect match to the guide at resonance; circle  $C$  with  $m^2R_{0b} < 1$  is said to be *undercoupled*; and circle  $B$  with  $m^2R_{0b} > 1$  is *overcoupled*. To match the last two, the coupling ratio  $m^2$  would have to be changed. As with the lumped resonant system, the value of  $Q_0$  can now be found from the specific value of  $\delta$  which reduces impedance magnitude at reference  $b$  by  $1/\sqrt{2}$  of its resonant value. On the Smith chart, this is the point  $R = X$  and the corresponding  $\delta$  may be denoted  $\delta_1$ . At this point the known quantities are  $\delta'_1$  corresponding to  $\delta_1$ ,  $m^2X$  found from (5),  $m^2R_{0b}$ , which is the value of  $Z_b$  at resonance, and  $2Q_0\delta_1 = 1$  in the denominator of (6). Then

$$Q_0 = \frac{1}{2\delta_1} \quad (9)$$

and (8) may be solved to find  $Q_0$  in terms of the known quantities.

The value of  $Q_0$  thus determined is the "unloaded  $Q$ " since it does not account for loading by the guide. A loaded  $Q$  which accounts for this is also used and may be found from Fig. 10.11b as

$$\frac{1}{Q_L} = \frac{G + m^2}{\omega_0 C} = \frac{1}{Q_0} + \frac{1}{Q_{\text{ext}}} \quad (10)$$

where "external  $Q$ ,"  $Q_{\text{ext}}$ , results from

$$Q_{\text{ext}} = \frac{\omega_0 C}{m^2} \quad (11)$$

It is assumed here that the generator is matched so that the impedance looking toward the guide is its characteristic impedance, taken here as unity.

## 10.12 RESONATOR PERTURBATIONS

In the condition of resonance, average stored magnetic and electric energies are equal. If a small perturbation is made in one of the cavity walls, this will in general change one type of energy more than the other, and resonant frequency would then shift by an amount necessary to again equalize the energies. Perturbation theory<sup>7</sup> shows the amount of frequency shift when a small volume  $\Delta V$  is removed from the resonator by pushing in the boundaries. This may be written

$$\frac{\Delta\omega}{\omega_0} = \frac{\int_{\Delta V} (\mu H^2 - \epsilon E^2) dV}{\int_V (\mu H^2 + \epsilon E^2) dV} = \frac{\Delta U_H - \Delta U_E}{U} \quad (1)$$

where  $\Delta U_H$  is the magnetic energy removed,  $\Delta U_E$  the electric energy removed, and  $U$  the total stored energy, all time averages. We illustrate with two examples.

### Example 10.12a

#### PERTURBATION OF RESONANT PARALLEL-PLANE LINE

We first take a simple case for which we can check the answer. Consider the parallel-plane transmission line of Fig. 10.12a, shorted at the two ends. The unperturbed resonance with the lowest frequency is at  $l = \lambda/2$  [Eq. 10.6(1)]:

$$\omega_0 = \frac{2\pi v_p}{\lambda} = \frac{\pi v_p}{l} \quad (2)$$

If we perturb by moving one end plate in by  $\Delta l$ , the new resonance is

$$(\omega_0 + \Delta\omega) = \frac{\pi v_p}{l - \Delta l} \approx \omega_0 \left( 1 + \frac{\Delta l}{l} \right) \quad (3)$$

<sup>7</sup> R. F. Harrington, *Time-Harmonic Electromagnetic Fields*, Chap. 7, McGraw-Hill, New York, 1961.

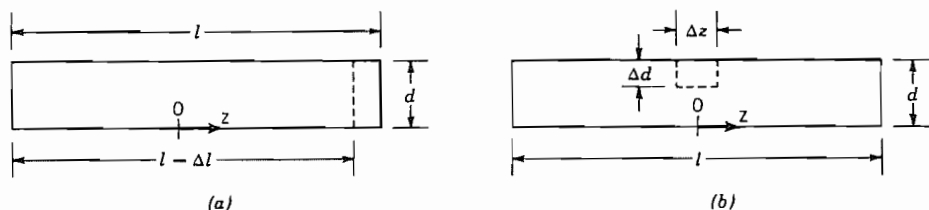


**FIG. 10.12** Parallel-plane transmission line with perturbations: (a) by decreasing length by  $\Delta l$ ; (b) by introducing a rectangular indentation at the center of the line.

In using the perturbation formula (1), only magnetic energy is removed. If unperturbed magnetic field is of the form

$$H_0(z) = H_0 \sin \frac{\pi z}{l} \quad (4)$$

Total stored energy (twice the average energy in magnetic fields) is

$$U = 2wd \int_{-l/2}^{l/2} \frac{\mu H_0^2}{4} \sin^2 \frac{\pi z}{l} dz = wld \frac{\mu H_0^2}{4} \quad (5)$$

where  $w$  is width of the line and  $d$  the spacing. The energy removed is

$$\Delta U_H = \frac{\mu H_0^2}{4} w d \Delta l \quad (6)$$

so by (1)

$$\frac{\Delta \omega}{\omega_0} = \frac{\Delta l}{l} \quad (7)$$

which agrees with (3).

Now suppose the perturbation is at the center of the line where only electric field is removed, as shown by the dashed outline in Fig. 10.12b. If unperturbed electric field is

$$E_0(z) = E_0 \cos \frac{\pi z}{l} \quad (8)$$

the total energy stored is

$$U = 2U_E = 2wd \int_{-l/2}^{l/2} \frac{\epsilon E_0^2}{4} \cos^2 \frac{\pi z}{l} dz = wld \frac{\epsilon E_0^2}{4} \quad (9)$$

And the electric energy removed is

$$\Delta U_E = w \Delta d \Delta z \frac{\epsilon E_0^2}{4} \quad (10)$$

so by (1)

$$\frac{\Delta\omega}{\omega_0} = -\frac{\Delta d \Delta z}{ld} \quad (11)$$

To check this, we may use the equivalent circuit of the capacitively loaded quarter-wave line shown in Fig. 10.12*b*. Resonance is given by

$$\omega\left(\frac{\Delta C}{2}\right) = Y_0 \cot\left(\frac{\omega l}{2v_p}\right) \quad (12)$$

where

$$\Delta C = \epsilon w \Delta z \left( \frac{1}{d - \Delta d} - \frac{1}{d} \right) \approx \frac{\epsilon w \Delta z \Delta d}{d^2} \quad (13)$$

If  $\omega = \omega_0 + \Delta\omega$  and  $\omega_0 l / v_p = \pi$ , to first order (12) gives

$$\frac{\Delta\omega}{\omega_0} \approx -\frac{\Delta C v_p}{l Y_0} = -\left( \frac{\epsilon w \Delta z \Delta d}{l d^2} \right) \left( \frac{1}{\mu \epsilon} \right)^{1/2} \left( \frac{\mu}{\epsilon} \right)^{1/2} \frac{d}{w} \quad (14)$$

This reduces to (11), including the check of sign.

### Example 10.12*b*

#### PERTURBATION ON BOTTOM OF CYLINDRICAL CAVITY

For a more practical example, imagine a small volume  $\Delta V$  taken out of the pillbox resonator of volume  $V_0$  in Fig. 10.12*c*, along the axis where electric field is maximum and magnetic field negligible. The change in energy stored is then

$$\Delta U_E \approx \frac{\epsilon E_0^2}{4} \Delta V \quad (15)$$

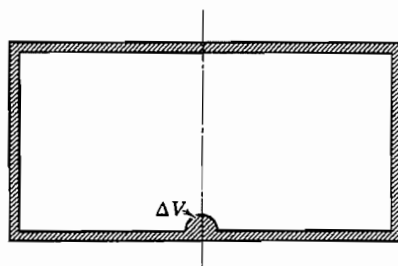


**FIG. 10.12*c*** Small perturbation in bottom of circular cylindrical cavity.

The total energy of the resonator is given by Eq. 10.5(5). Frequency shift from (1) for the lowest mode with  $ka = 2.405$  is then

$$\frac{\Delta\omega}{\omega_0} = -\frac{\epsilon E_0^2 \Delta V}{2\pi\epsilon dE_0^2 a^2 J_1^2(ka)} = -1.85 \frac{\Delta V}{V_0} \quad (16)$$

The shift in resonant frequency determines the ratio  $E_0^2/U$  needed for determination of  $R_0/Q$ . Frequency shifts can be measured accurately, and the perturbation can be made in the form of a small conducting bead moved by an insulating thread along the axis. Field can be measured at all points on the axis, and thus its integral found even when field cannot be assumed to be uniform across the gap.

### 10.13 DIELECTRIC RESONATORS

We saw in the earlier sections of this chapter that a section of a hollow metal waveguide shorted at the ends constitutes a resonant structure with properties similar to resonant  $L$ - $C$  circuits. Similarly, a section of dielectric waveguide (Sec. 9.2) exhibits resonances and can be used for the same purposes. Some materials have very high permittivities and wave energy is therefore strongly confined within the material. Wavelength is small so the dielectric resonator can be much smaller than an empty hollow metal structure. Early work<sup>8</sup> employed high-purity  $\text{TiO}_2$  ceramic material with  $\epsilon_r \approx 100$  and  $\epsilon''/\epsilon' \approx 10^{-4}$ . Values of  $Q$  (not accounting for losses in supporting structures) then are high (about  $10^4$ ) as shown in Prob. 10.3d. The difficulty with  $\text{TiO}_2$  is that its  $\epsilon_r$  has an intolerably strong temperature dependence of  $10^3$  parts per million (ppm) per degree Celsius, which leads to a resonant frequency dependence of 500 ppm/°C. More recently, ceramics have been developed<sup>9</sup> that can be made with temperature coefficients selected to offset those of the supporting structures, giving a net zero temperature dependence. These have  $\epsilon_r \approx 37.5$  and  $\epsilon''/\epsilon' \approx 2 \times 10^{-4}$  at about 10 GHz. Disks of these materials can conveniently be introduced as resonators into microwave-integrated circuits and use beyond 100 GHz is expected.

Exact analysis is possible for a sphere and a toroid, but shapes of greater technical interest such as rectangular prisms, disks, and rods must be treated approximately. It is seen that fields at the surface of a region of very high permittivity satisfy approximately the so-called *open-circuit* boundary condition for which the normal component of electric field and the tangential component of magnetic field are zero. This is made plausible by considering reflections of a plane wave in going from a dielectric of high permittivity (low intrinsic impedance) to one of low permittivity (high intrinsic impedance). One could calculate the resonant frequency of a dielectric resonator by surrounding it with a contiguous perfect magnetic conductor to impose the above stated conditions. How-

<sup>8</sup> S. B. Cohn, IEEE Trans. Microwave Theory Tech. **MTT-16**, 218 (1968).

<sup>9</sup> M. R. Stiglitz, Microwave J. **24**, 19 (1981).



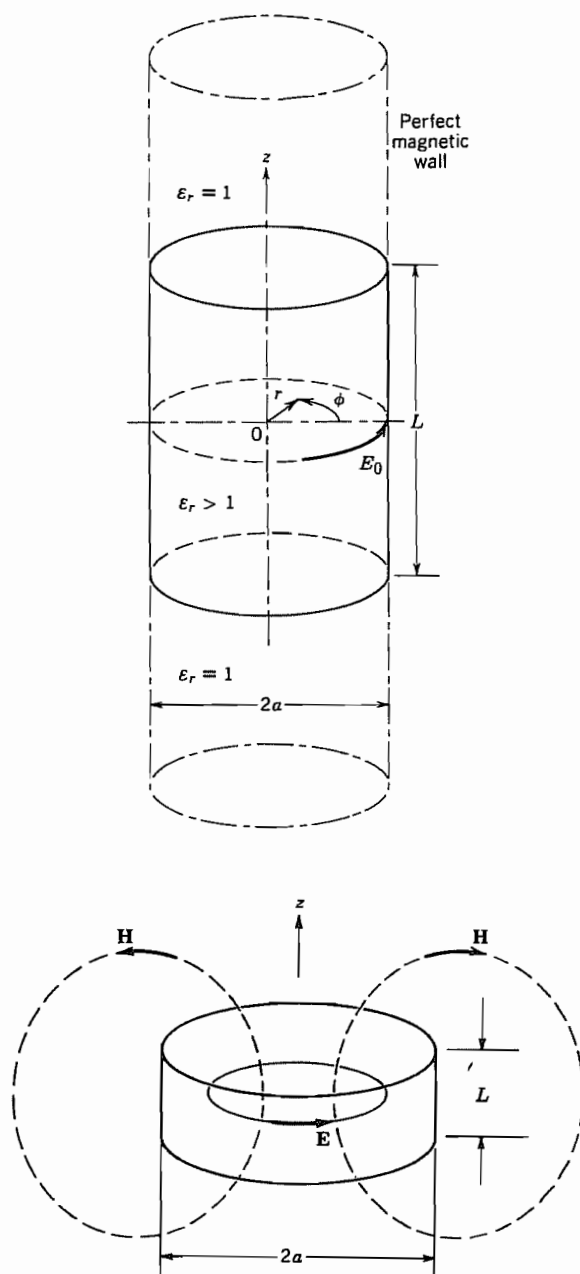


**FIG. 10.13** (a) Dielectric cylinder in magnetic-wall waveguide boundary. (b) Lowest-order mode where  $L \lesssim 2a$  in dielectric resonator. Fields  $\mathbf{H}$  outside  $r = a$  are extensions of those given by model in (a).

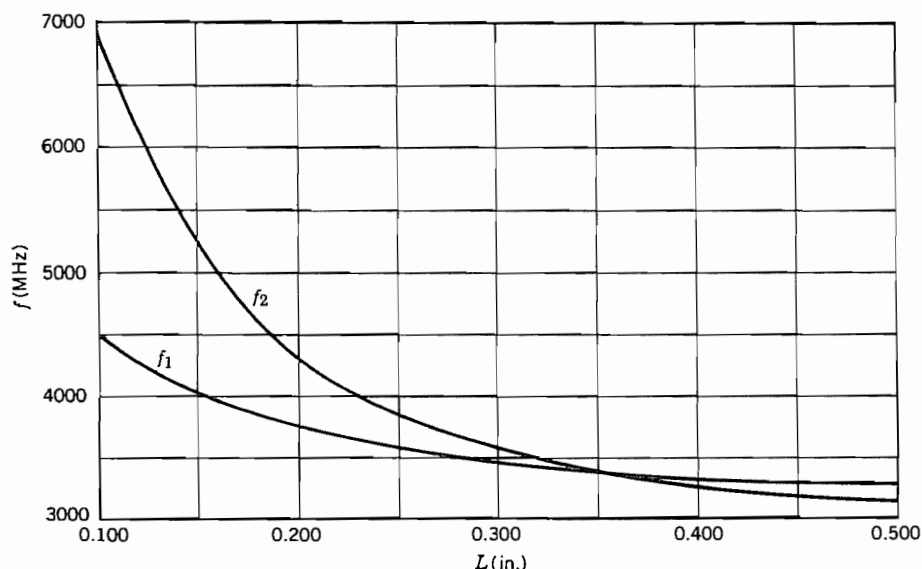


**FIG. 10.13c** Experimental data on the lowest resonant frequencies versus length of a dielectric cylinder of circular cross section. Radius  $a = 0.162$  in. After S. B. Cohn, *IEEE Trans. Microwave Theory Tech.* **MTT-16**, 218 (1968). © 1968 IEEE.

ever, since the open-circuit boundary conditions are only approximately satisfied for finite-permittivity resonators, modifications in the use of the perfect magnetic boundary have been found to give better results. The two lowest-order modes for circular cylindrical disks and rods are one with zero electric field along the axis and one with zero magnetic field along the axis. The model for the former places the solid dielectric cylinder inside a contiguous infinitely long, magnetic cylindrical waveguide so that the open-circuit conditions are imposed only on the cylindrical surface as in Fig. 10.13a. The model for the mode with zero magnetic field along the axis imposes the open-circuit condition only on the end faces of the dielectric cylinder by means of infinite parallel magnetic conducting plates. In either case the resonant fields and frequency are found by setting up propagating-type solutions of the wave equation inside and attenuating fields outside the dielectric and matching boundary conditions. The result is that the mode with zero axial electric field has the lowest resonant frequency for dielectric cylinders with length less than the diameter. The field distribution for this mode is shown in Fig. 10.13b. Some experimental results are shown in Fig. 10.13c. The curve labeled  $f_1$  is the mode with zero axial electric field and  $f_2$  has zero axial magnetic field. A general treatment of arbitrary shapes of dielectric resonators is given by Van Bladel.<sup>10</sup>

<sup>10</sup> J. Van Bladel, *IEEE Trans. Microwave Theory Tech.* **MTT-23**, 199 (1975).

**Example 10.13****TE MODE IN DIELECTRIC RESONATOR**

As an example we do the analysis for the case with the circular cylinder of dielectric enclosed in a perfectly conducting magnetic waveguide shown in Fig. 10.13a. Use is made of the concept of duality (Sec. 9.5) in which  $\mathbf{E}$  is replaced by  $\mathbf{H}$ ,  $\mathbf{H}$  by  $-\mathbf{E}$ ,  $\mu$  by  $\epsilon$ , and  $\epsilon$  by  $\mu$  in known field distributions to find another solution of Maxwell's equations that fits boundary conditions dual to those of the given field. The circular waveguide modes in Sec. 8.9 can be adapted. In particular, the TM mode with an electric boundary becomes a TE mode with the magnetic boundary. The  $H_\phi$  component in Eq. 8.9(9) becomes the  $E_\phi$  component and can be written as

$$E_\phi = E_0 \frac{J_1(k_c r)}{J_1(p_{01})} e^{-j\beta_d z}, \quad |z| \leq \frac{L}{2} \quad (1)$$

where the propagation factor is included for a wave in the  $+z$  direction and the subscript  $d$  signifies the dielectric region. Taking account of waves in both directions in the dielectric, one has

$$E_\phi = 2E_0 \frac{J_1(k_c r)}{J_1(p_{01})} \cos \beta_d z, \quad |z| \leq \frac{L}{2} \quad (2)$$

The frequency is assumed low enough that the waves outside the dielectric ( $|z| > L/2$ ) are cut off. Choosing the coefficient to ensure continuity of  $E_\phi$  across the end of the dielectric, we may write

$$E_\phi = 2E_0 \frac{J_1(k_c r)}{J_1(p_{01})} \cos \frac{\beta_d L}{2} e^{-\alpha_a(|z| - L/2)}, \quad |z| \geq \frac{L}{2} \quad (3)$$

The magnetic field components tangential to the end faces of the dielectric are

$$H_r = j \frac{\beta_d}{\omega \mu} 2E_0 \frac{J_1(k_c r)}{J_1(p_{01})} \sin \beta_d z, \quad |z| \leq \frac{L}{2} \quad (4)$$

$$H_r = \pm \frac{j\alpha_a}{\omega \mu} 2E_0 \frac{J_1(k_c r)}{J_1(p_{01})} \cos \beta_d \frac{L}{2} e^{-\alpha_a(|z| - L/2)}, \quad |z| \geq \frac{L}{2} \quad (5)$$

where we have used the relation dual to Eq. 8.9(9). The upper sign in (5) applies at  $z = L/2$  and the lower at  $z = -L/2$ . Then, equating  $H_r$  across the dielectric boundary at  $z = \pm L/2$  we find the determinantal relation for the resonant frequency:

$$\beta_d \tan \frac{\beta_d L}{2} = \alpha_a \quad (6)$$

where

$$\beta_d = \sqrt{\frac{\omega^2 \epsilon_r}{c^2} - \left(\frac{p_{01}}{a}\right)^2} \quad (7)$$

and

$$\alpha_a = \sqrt{\left(\frac{p_{01}}{a}\right)^2 - \left(\frac{\omega}{c}\right)^2} \quad (8)$$

These calculations give resonant frequencies about 10% lower than the experimental data in the range  $0.24 < L/2a < 0.62$ .

## PROBLEMS

- 10.2a** An analogy can be made between acoustic resonances in a closed box with fixed walls and electromagnetic resonances in a box with walls of high conductivity. Develop the comparison further, stressing similarities and differences.
- 10.2b** Show that the mode described in Sec. 10.2 (resonant condition and field expressions) would be obtained if one started with the point of view that it was a  $TE_{10}$  mode propagating in the  $x$  direction; similarly consider it a  $TM_{11}$  mode propagating in the  $y$  direction exactly at cutoff.
- 10.2c** Find the total charge on the top plate and bottom plate for the resonator of Sec. 10.2. Determine an equivalent capacitance that would give this charge with a voltage equal to that between top and bottom at the center of the box. Compare this equivalent capacitance with the parallel-plate capacitance of the top and bottom plates with fringing neglected.
- 10.2d** Find the total current in the side walls of the resonator of Sec. 10.2. Determine an equivalent inductance in terms of this current and the magnetic flux linking a vertical path at the center of the box. What resonant frequency would be given by this inductance and the equivalent capacitance of Prob. 10.2c? Compare with result of Eq. 10.2(1).
- 10.2e** Suppose that in place of a perfect conductor at  $z = d$ , a "reactive wall" giving a wave reactance  $E_y/H_x = jX$  is placed there. Obtain the condition for resonance. Discuss physical ways in which the reactance wall might be produced, at least as an approximation.
- 10.3a** Calculate the maximum energy stored in magnetic fields for the simple mode of the rectangular resonator and show that it is the same as Eq. 10.3(1).
- 10.3b** Convert the phasor forms of electric and magnetic fields of Sec. 10.2 to instantaneous forms and find stored electric and magnetic energy as functions of time. Show that the sum is a constant equal to the value of Eq. 10.3(1).
- 10.3c** From the definition of  $Q$  in terms of energy storage and power loss, Eq. 10.3(3), show that the decay of energy in a natural oscillation after excitation is removed is of the form  $\exp(-t/\tau)$  where  $\tau = Q/\omega_0$ . How many periods of oscillation are there in the  $1/e$  time of the decay?
- 10.3d** For an imperfect dielectric, show that the  $Q$  for any resonant mode is just  $\epsilon'/\epsilon''$ , neglecting losses of the conducting walls. Give the value for the dielectrics of Table 6.4a at 10 GHz and compare with the value of  $Q$  for a copper cube-shaped cavity given in the text.

- 10.3e** Modify the expression 10.3(2) for wall losses if front and back are of one material with surface resistivity  $R_{s1}$ , the two sides of another with  $R_{s2}$ , and top and bottom of a third material with  $R_{s3}$ . Give the special case of this for a cube.
- 10.3f** Suppose that a perfect dielectric were available with  $\epsilon' = 5\epsilon_0$ . How would the  $Q$  of a dielectric-filled cube compare with that of an air-filled one for the simple mode studied? Why are they different? (Compare for the same resonant frequency in both cases.)
- 10.3g** A square cavity resonator utilizing the simple  $TE_{101}$  mode is to be designed for a millimeter-wave electron device for operation at  $f = 0.3$  THz. Height of the cavity must be kept small (0.1 mm) to minimize electron transit time. The dielectric in the copper cavity is vacuum and the cross section is square. Calculate cavity size, the  $Q$ , and bandwidth. Also calculate the shunt resistance  $R_0 = (E_0 b)^2 / 2W_L$ , which is a measure of the interaction of the electron beam with the cavity. Note that more advantageously shaped cavities, such as that in Fig. 10.9a, have much higher impedances; for example, see Prob. 10.9c.
- 10.4a** For  $TE_{mnp}$  and  $TM_{mnp}$  modes in a cubic resonator, consider combinations of the integers with no integer higher than 2. How many *different* resonant frequencies do these represent? What is the degree of degeneracy (number of modes at a given frequency) for each frequency? (Note carefully which, if any, integers may be zero.)
- 10.4b\*** By combining incident and reflected waves as was done for the  $TE_{101}$  mode of Sec. 10.2, find electric and magnetic field expressions of the  $TE_{111}$  mode of the rectangular box. Sketch field distributions in the three coordinate planes. Find the expression for  $Q$  if conductors are imperfect.
- 10.4c** Derive the expression for  $Q$  of a  $TE_{mmmm}$  mode in a cube  $a = b = d$  and show that it increases as  $m$  increases for a given dielectric and resonant frequency. Explain the result.
- 10.5a** Find expressions for resonant frequency in terms of length and radius for the  $TM_{021}$  and  $TM_{111}$  modes of a circular cylindrical cavity.
- 10.5b** A circular resonator has height  $h$  and radius  $a$ . Give the lowest resonant frequency for which a degeneracy between two modes occurs and the designations of these modes. Make rough sketches of the field patterns. How might a small perturbation be added to change the resonant frequency of one mode but not of the other?
- 10.5c** Plot curves of  $d/\lambda$  versus  $a/d$  for all the significant modes in a circular cylindrical cavity over the range  $0 < d/\lambda < 2$ ,  $0 < a/d < 5$ . Note especially ranges of operation where there is only one mode over a considerable region of operation.
- 10.5d\*** Give the field components and obtain expressions for energy storage, power loss, and  $Q$  for the  $TM_{011}$  mode of a circular cylindrical resonator.
- 10.5e\*** Repeat Prob. 10.5d for the  $TE_{011}$  mode.
- 10.6a** Show that the resonant frequency of an open-circuited microstrip resonator as in Fig. 10.6b with  $w = 0.2$  mm,  $d = 0.5$  mm,  $l = 5$  mm, and  $\epsilon_r = 9.8$ , taking account of end corrections but using the static value of  $\epsilon_{eff}$ , is 11.43 GHz. What fractional error is incurred if the end correction is neglected? Estimate the error in the lowest resonant frequency resulting from neglecting dependence of  $\epsilon_{eff}$  on frequency?
- 10.6b\*** Assume that the conductors in the resonator in Prob. 10.6a are copper and are  $2.5 \mu\text{m}$  thick.

- (i) Calculate the  $Q$  for the lowest mode, accounting for metal and dielectric losses using Eq. 5.14(5) and Sec. 8.6. Use a static value of  $\epsilon_{\text{eff}}$ .
- (ii) Calculate the  $Q_{\text{rad}}$  associated with radiation losses using Eq. (11.14) of Hoffmann<sup>1</sup>, which is

$$Q_{\text{rad}} = \frac{3Z_0\epsilon_{\text{eff}}}{16\eta_0(df_0/c)^2}$$

Also calculate the total  $Q$ , including  $Q_{\text{rad}}$  and that associated with the dielectric and conductor losses in part (i). By what percentage is the  $Q$  of part (i) lowered by radiation for this particular resonator.

- 10.6c** Design a coplanar waveguide ring resonator with fundamental resonance at 4.0 GHz on an alumina substrate ( $\epsilon_r = 9.8$ ) having thickness  $d = 1$  mm. Choose the strip width  $w = 0.1$  mm and the total gap  $a = 0.2$  mm. See Fig. 8.6e. Calculate the mean diameter of the ring and sketch the structure in a manner similar to Fig. 10.6c, but with capacitive input and output coupling. Make the calculation using  $\epsilon_{\text{eff}}(0)$  and then calculate the percentage change of resonant frequency if the frequency dependence of  $\epsilon_{\text{eff}}$  is included.
- 10.6d** Find the four lowest resonant frequencies in a rectangular patch antenna having parameters  $a = 5$  mm,  $b = 6$  mm,  $d = 0.635$  mm, and  $\epsilon_r = 2.5$ . (See Fig. 10.6d.)
- 10.6e** Find the dependence of  $Q$  (neglecting radiation) on order numbers  $m$  and  $n$  for a given resonant frequency in a rectangular patch resonator of fixed materials. Review the discussion General Comments in Sec. 10.4 for the rectangular box cavity and discuss your result for the patch resonator in comparison with the box cavity. What is the approximate dependence of radiation  $Q$  on the mode numbers?
- 10.6f** Find the lowest three resonant frequencies in a circular patch resonator with radius  $a = 1$  cm, dielectric thickness  $d = 0.6$  mm, and permittivity  $\epsilon_r = 11$ .
- 10.6g** Calculate the quality factor  $Q_c$  (accounting for only the conductor losses) for the mode with the lowest resonant frequency in the resonator in Prob. 10.6d, assuming niobium superconductor metallization with operation at 4.2 K. If the niobium were replaced by copper, what would be the  $Q_c$  at 4.2 K, assuming for copper that  $\sigma(4.2 \text{ K})/\sigma(300 \text{ K}) = 5$ .
- 10.6h** Show where slits may be cut in the circular patch resonator to suppress  $\text{TM}_{n10}$  modes with  $n \neq 0$ . Explain your reasoning. Is it possible to suppress  $\text{TM}_{010}$  modes without suppressing the  $\text{TM}_{110}$  modes? Why?
- 10.7** Develop the TE set of spherical waves, Eq. 10.7(20), starting from Maxwell's equations with no  $\phi$  variations, in parallel to the development for the TM set.
- 10.8a** By utilizing solutions and definitions of Sec. 10.7 write expressions for the components in a spherical TE mode with  $n = 2$  in terms of sines and cosines.
- 10.8b\*** Determine the  $Q$  of the  $\text{TE}_{101}$  mode in the spherical resonator.
- 10.9a** A coaxial line of radii 0.5 and 1.5 cm is loaded by a gap capacitance as in Fig. 10.9a of 1 pF. Find the length  $l$  for resonance at 3 GHz.
- 10.9b** A radial line of spacing  $h = 1$  cm has a central post as in Fig. 10.9c of radius 0.5 cm and capacitance 1 pF. Find the radius  $r_2$  for resonance at 3 GHz.
- 10.9c** Obtain expressions for the  $Q$  and the impedance referred to the gap ( $V^2/2W_L$  where  $V$  is gap voltage) for the resonator of Fig. 10.9a, neglecting losses in region B. Calcul-

late values for a copper conductor and the data of Prob. 10.9a. Compare with the value  $R_0 = 3.1 \times 10^4 \Omega$  found for the square cavity resonator in Prob. 10.3g and comment on difference if used for interaction with an electron beam.

- 10.9d** Find  $Q$  and impedance if in addition to copper losses there are losses in region  $B$  representable by a shunt resistance  $R_{sh}$ . Repeat the numerical calculation of Prob. 10.9c, taking  $R_{sh} = 10,000 \Omega$ .
- 10.9e** For a cone angle  $\theta_0$  of 15 degrees in Fig. 10.9e, find radius  $a$  for resonance at 3 GHz if center capacitance is 1 pF.
- 10.9f** For the conical resonator with no loading capacitance, show that there is a value of  $\theta_0$  which gives maximum  $Q$ . Calculate the value of  $Q$  for a copper resonator designed for  $\lambda_0 = 15$  cm with this optimum angle.
- 10.10a** For the simple mode in a rectangular resonator perform an approximate analysis as in Ex. 10.10 leading to an expression for input impedance of a loop introduced at the center of a side wall.
- 10.10b** For the  $TM_{010}$  mode in the circular cylindrical resonator, suppose that the coupling to the line is by means of a small probe of length  $d'$  extending axially from the bottom center. Taking voltage induced in the probe as the probe length multiplied by electric field of the mode, find an expression for input admittance at resonance of the unperturbed mode, utilizing a procedure similar to that of Ex 10.10. The probe capacitance is  $C$ .
- 10.10c** For a circular cylindrical cavity of radius 10 cm, height 10 cm, resonant in the  $TM_{010}$  mode, find the approximate resistance coupled into a transmission line by a loop of area  $1 \text{ cm}^2$  introduced at the position of maximum magnetic field. Repeat for a probe of length 1 cm introduced at the position of maximum electric field.
- 10.11a** For a cavity with  $m^2 R_{0b} = 2$  and  $Q_0 = 5000$ , plot the locus of impedance on the Smith chart as  $\delta$  is varied, showing selected values of  $\delta$  on the locus. Modify  $m^2$  to yield critical coupling and repeat.
- 10.11b** Plot standing wave ratio in the guide versus  $\delta$  for both parts of Prob. 10.11a. Describe how one might use the plot of SWR versus  $\delta$  to determine  $Q$  as an alternate to the impedance function.
- 10.11c** Find  $Q_L$  and  $Q_{ext}$  for Prob. 10.11a with  $\beta l = 0.3$  radian.
- 10.11d** When coupling to an electron stream, as in a klystron cavity such as described in Sec. 10.10, gain is proportional to  $R_0$  and bandwidth to  $1/Q$ , so the parameter  $R_0/Q$  is useful in describing the effect of the cavity on gain-bandwidth product. Assuming electric field  $E_0$  is uniform across the coupling gap of width  $d$ , show that  $R/Q = (E_0 d)^2 / 2\omega_0 U$ . Discuss ways in which  $E_0^2/U$  might be measured.
- 10.11e** Find  $R_0/Q$  for a pillbox resonator of the type studied in Sec. 10.5 operating in its lowest mode. Frequency is 10 GHz and  $d = 0.5$  cm. The conductor is copper.
- 10.11f** Derive the expression for  $R_0/Q$  for the small-gap coaxial line resonator pictured in Fig. 10.9a.
- 10.12a** Obtain the approximate expression for frequency shift in a circular cylindrical cavity if small volume  $\Delta V$  is taken from the side wall for the  $TM_{010}$  mode where magnetic field is large and electric field small.
- 10.12b\*** Discuss qualitatively the effects of a thin dielectric rod along the axis of a pillbox cavity, a thin dielectric sheet along the bottom of the cavity, and a dielectric bead

introduced along the axis of the cavity. (Note that the first two problems can be solved exactly.)

- 10.12c\*** Consider a periodic circuit as in Fig. 9.10a with parallel perfectly conducting planes extending from  $x = 0$  to  $x = a$  at  $z = d/2$  and  $z = (n + \frac{1}{2})d$  where  $n$  is an integer. Discuss resonance for such a system. Will there be a resonance corresponding to each of the space harmonics defined in Sec. 9.10? Show how measurement of the number of nodes (voltage minima) between planes as frequency is changed permits plotting of the  $\omega$ - $\beta$  diagram.
- 10.13** A dielectric resonator with zero axial electric field has radius  $a = 0.162$  in.,  $\epsilon_r = 100$ , and is to be resonant at 3.5 GHz. Use Eqs. 10.13(6) and (7) to estimate length and compare with the experimental curve of Fig. 10.13c. What would be the estimated length if a magnetic short were used on the ends as well as on the side walls?